Branch cuts of Stokes wave on deep water. Part II: Structure and location of branch points in infinite set of sheets of Riemann surface

Pavel M. Lushnikov†

Department of Mathematics and Statistics, University of New Mexico, Albuquerque, MSC01 1115, NM, 87131, USA

(Received 14 September 2015)

Stokes wave is a finite amplitude periodic gravity wave propagating with constant velocity in inviscid fluid. Complex analytical structure of Stokes wave is analyzed using a conformal mapping of a free fluid surface of Stokes wave into the real line with fluid domain mapped into the lower complex half-plane. There is one square root branch point per spatial period of Stokes located in the upper complex half-plane at the distance v_c from the real axis. The increase of Stokes wave height results in approaching v_c to zero with the limiting Stokes wave formation at $v_c = 0$. The limiting Stokes wave has 2/3 power law singularity forming $2\pi/3$ radians angle on the crest which is qualitatively different from the square root singularity valid for arbitrary small but nonzero v_c making the limit of zero v_c highly nontrivial. That limit is addressed by crossing a branch cut of square root into the second and higher sheets of Riemann surface to find coupled square root singularities at the distances $\pm v_c$ from the real axis at each sheet. The number of sheets is infinite and the analytical continuation of Stokes wave into all these sheets is found together with the series expansion in half-integer powers at $\pm v_c$ singular points within each sheet. It is conjectured that non-limiting Stokes wave at the leading order consists of the infinite number of nested square root singularities. These nested square roots form 2/3 power law singularity of the limiting Stokes wave as v_c vanishes.

Key words:

1. Introduction

In Part I (Dyachenko *et al.* 2015*b*), we obtained Stokes wave solution numerically with high precision and analyzed that solution using Padé approximation. We showed a convergence of Padé approximation of Stokes wave to a single branch cut per spatial period in the upper complex half plane $\mathbb{C}^+$ of the axillary complex variable w. In this paper we formulate the nonlinear integral equation for the jump of Stokes wave at the branch cut in the physical (first) sheet of Riemann surface. We show that the Riemann surface of Stokes has infinite number of sheets as sketched in Figure 1 and study the structure of singularities in these sheets.

Stokes wave is the fully nonlinear periodic gravity wave propagating with the constant velocity c (Stokes 1847, 1880*a*). It corresponds to two-dimensional potential flow of an ideal incompressible fluid. Following Part I (Dyachenko *et al.* 2015*b*), we use scaled units

† Email address for correspondence: plushnik@math.unm.edu

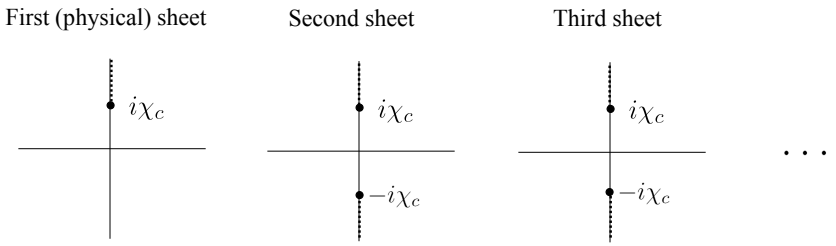

FIGURE 1. A schematic of Riemann surface sheets for non-limiting Stokes wave in a complex variable ζ (1.6) near the origin. First (physical) sheet has a square-root singularity at $\zeta = \mathrm{i}\chi_c$ only in the upper complex half-plane $\mathbb{C}^+$ with the the lower complex half-plane $\mathbb{C}^-$ corresponding to the domain occupied by the fluid. Other (non-physical) sheets have square-root singularities at $\zeta = \pm\mathrm{i}\chi_c$. Other square-root singularities are possible beyond the disks of convergence $|\zeta \pm \mathrm{i}\chi_c| < 2\chi_c$ in sheets beyond the first and the second sheets. Dashed lines show branch cuts. In addition there are the singularities at $\zeta = \pm\mathrm{i}$ in all sheets which corresponds to $w = \infty$.

at which $c = 1$ for the linear gravity waves and the spatial period is $\lambda = 2\pi$. Nonlinearity of Stokes wave increases with the increase of H/λ, where H is the Stokes wave height which is defined as the vertical distance from the crest to the trough of Stokes wave. Stokes wave has $c > 1$ and $H \to 0$, $c \to 1$ correspond to the limit of linear gravity wave. The Stokes wave of the greatest height $H = H_{max}$ (also called by the limiting Stokes wave) has the singularity in the form of the sharp angle of $2\pi/3$ radians on the crest (Stokes 1880*b*). We assume that singularity touches the fluid surface at $w = 0$ and that for the limiting Stokes wave at $w \to 0$ there is the following expansion

$$z(w) = \mathrm{i}\frac{c^2}{2} - \mathrm{i}\left(\frac{3c}{2}\right)^{2/3} (\mathrm{i}w)^{2/3} + \text{h.o.t.} \tag{1.1}$$

which ensures the sharp angle of $2\pi/3$ radians on the crest. Equation (1.1) recovers the result of Stokes (1880*b*). Here h.o.t. means higher order terms which approaches 0 faster than $w^{2/3}$ as $w \to 0$. Also

$$z(w) = x(w) + \mathrm{i}y(w) \tag{1.2}$$

is the conformal transformation which maps a half-strip $-\pi \leqslant u \leqslant \pi$, $-\infty < v \leqslant 0$ of the conformal variable

$$w = u + \mathrm{i}v \tag{1.3}$$

into a fluid domain of infinite depth $-\infty < y \leqslant \eta(x)$, $-\pi \leqslant x \leqslant \pi$ of the complex plane z (see Fig. 1 of Part I (Dyachenko *et al.* 2015*b*)). Here x and y are the horizontal and vertical physical coordinates, respectively. $y = \eta(x)$ is the surface elevation in the reference frame moving with the speed c. As discussed in details in Part I (Dyachenko *et al.* 2015*b*), choosing

$$z(w) = w + \tilde{z}(w), \tag{1.4}$$

with $x(w) = u + \tilde{x}(w)$ and $\tilde{y}(w) = v + y(w)$, ensures that $\tilde{z}(w)$ is 2π-periodic function

$$\tilde{z}(w + 2\pi) = \tilde{z}(w), \quad \tilde{x}(\pm\pi) = 0. \tag{1.5}$$

It was found by Grant (1973) that the corner singularity (1.1) might not be a simple algebraic branch point because next order term in the expansion (1.1) might be a power of the transcendental number. The existence of limiting Stokes wave with the jump of the slope at the crest in $2\pi/3$ radians was independently proven by Plotnikov (1982) and Amick *et al.* (1982).

In this paper we focus on analyzing singularities of near-limiting Stokes wave. Grant (1973) showed that assuming that singularity is a power law branch point, then that singularity has to have a square-root form to the leading order. Tanveer (1991) provided much stronger result proving that the only possible singularity in the finite complex upper half-plane is of square-root type. The existence of only one square-root singularity per period in a finite physical complex plane was also confirmed in Part I (Dyachenko *et al.* 2015*b*) and (Dyachenko *et al.* 2014) by analyzing the numerical solution for Stokes wave.

We now consider an additional conformal transformation between the complex plane $w = u + \mathrm{i}v$ and the complex plane for the new variable

$$\zeta = \tan\left(\frac{w}{2}\right) \tag{1.6}$$

which maps the strip $-\pi < Re(w) < \pi$ into the complex ζ plane. In particular, the line segment $-\pi < w < \pi$ of the real line $w = u$ maps into the entire real line $(-\infty, \infty)$ in the complex ζ-plane as shown in Fig. 5 of Part I (Dyachenko *et al.* 2015*b*). Vertical half-lines $w = \pm\pi + \mathrm{i}v,\ 0 < v < \infty$ are mapped into a branch cut $\mathrm{i} < \zeta < \mathrm{i}\infty$. In a similar way, vertical half-lines $w = \pm\pi + \mathrm{i}v,\ -\infty < v < 0$ are mapped into a branch cut $-\mathrm{i}\infty < \zeta < \mathrm{i}$. However, $2\pi-$periodicity of $\tilde{z}(w)$ (1.5) allows to ignore these two branch cuts because $\tilde{z}(w)$ is continuous across them. Complex infinities $w = \pm\mathrm{i}\infty$ are mapped into $\zeta = \pm\mathrm{i}$. An unbounded interval $[\mathrm{i}v_c, \mathrm{i}\infty)$, $v_c > 0$ is mapped into a finite interval $[\mathrm{i}\chi_c, \mathrm{i})$ with

$$\chi_c = \tanh\frac{v_c}{2}. \tag{1.7}$$

The transformation (1.6) takes care of $2\pi-$periodicity of Stokes wave so that the function $z(\zeta)$ defined in the complex plane $\zeta \in \mathbb{C}$ corresponds to the function $z(w)$ defined in the strip $-\pi < Re(w) = u < \pi$. Here and below we abuse notation and use the same symbol z for both functions of ζ and w (and similar for other symbols). The additional advantage of using the mapping (1.6) is the compactness of the interval $(\mathrm{i}\chi_c, \mathrm{i})$ as mapped from the infinite interval $(\mathrm{i}v_c, \mathrm{i}\infty)$. Note that the mapping (1.6) is different from the commonly used (see e.g. Schwartz (1974); Tanveer (1991); Williams (1981)) mapping $\zeta = \exp(-\mathrm{i}w)$ (maps the strip $-\pi \leqslant Re(w) < \pi$ into the unit circle). That exponential mapping to the circle leaves the interval $(\mathrm{i}v_c, \mathrm{i}\infty)$ infinite in ζ plane.

The main result of this paper is that it was found an infinite number of sheets of Riemann surface with square root branch points located at $\zeta = \pm\mathrm{i}\chi_c$ starting from the second sheet (the first sheet has the singularity only at $\zeta = \mathrm{i}\chi_c$). At each sheet (except the first one) these singularities are coupled through complex conjugated terms which appear in the equation for Stokes wave. In contrast, the only singularity at $\zeta = \mathrm{i}\chi_c$ of the first sheet (besides the singularity at $\zeta = \mathrm{i}$) does not have a complex conjugated sister at $\zeta = -\mathrm{i}\chi_c$ which makes that (physical) sheet distinct from all others. It is conjectured that the leading order form of non-limiting Stokes wave has the form of the infinite number of nested square root singularities. These nested square roots form 2/3 power law singularity of the limiting Stokes wave as $\chi_c \to 0$.

The paper is organized as follows. In Section 2 a closed nonlinear integral equation for Stokes wave through the density at the branch cut is derived. Section 3 provides an alternative form for the equation of Stokes wave. Section 4 uses that alternative form to find an asymptotic of both Stokes wave at $Im(w) \to +\infty$ and the jump at branch cut. Section 5 discusses a numerical procedure to analyze the structure of sheets of Riemann surface for Stokes wave by the integration of the corresponding nonlinear ordinary differential equation (ODE). Section 6 derives the analytical expressions for coupled series expansions at $\zeta = \pm i\chi_c$ to reveal the structure of Riemann surface for Stokes wave. Section 7 analyzes possible singularities of Stokes in all sheets of Riemann surface and concludes that the only possible singularity for finite value of w is the square root branch point. Section 8 provides a conjecture on recovering of 2/3 power law of limiting Stokes wave from an infinite number of nested square root singularities of non-limiting Stokes wave in the limit $\chi_c \to 0$. In Section 9 the main results of the paper are discussed. Appendix A shows the equivalence of two forms of equation for Stokes wave used in the main text. Appendix B relates different forms of equation for Stokes wave in the rest frame and in the moving frame. Appendix C provides tables of the numerical parameters for Stokes wave.

2. Closed integral equation for Stokes wave through the density at the branch cut

The equation for Stokes wave used in Part I (Dyachenko *et al.* 2015*b*) is defined at the real line $w = u$ as follows

$$-c^2 y_u + y y_u + \hat{H}[y(1 + \tilde{x}_u)] = 0, \tag{2.1}$$

where

$$\hat{H} f(u) = \frac{1}{\pi} \text{p.v.} \int_{-\infty}^{+\infty} \frac{f(u')}{u' - u} \mathrm{d}u' \tag{2.2}$$

is the Hilbert transform with p.v. meaning a Cauchy principal value of integral. The Hilbert operator $\hat{H}$ transforms into the multiplication operator

$$(\hat{H} f)_k = \mathrm{i}\,\mathrm{sign}\,(k)\, f_k, \tag{2.3}$$

for the Fourier coefficients (harmonics) f_k,

$$f_k = \frac{1}{\lambda 2\pi} \int_{-\pi}^{\pi} f(u) \exp\left(-\mathrm{i}ku\right) \mathrm{d}u, \tag{2.4}$$

of the periodic function $f(u) = f(u + 2\pi)$ represented through the Fourier series

$$f(u) = \sum_{k=-\infty}^{\infty} f_k \exp\left(\mathrm{i}ku\right). \tag{2.5}$$

Here $\mathrm{sign}(k) = -1, 0, 1$ for $k < 0,\ k = 0$ and $k > 0$, respectively. Equation (2.5) implies that

$$\hat{H}^2 f = -(f - f_0), \tag{2.6}$$

where f_0 is the zeroth Fourier harmonic of f.

It is convenient to decompose the Fourier series (2.5) as follows

$$f(u) = f^+(u) + f^-(u) + f_0, \tag{2.7}$$

where

$$f^+(w) = \sum_{k=1}^{\infty} f_k \exp(\mathrm{i}kw) \tag{2.8}$$

is the analytical function in $\mathbb{C}^+$ and

$$f^-(w) = \sum_{k=-\infty}^{-1} f_k \exp(\mathrm{i}kw) \tag{2.9}$$

is the analytical function in $\mathbb{C}^-$. Then equation (2.3) implies that

$$\hat{H}f = \mathrm{i}(f^+ - f^-). \tag{2.10}$$

Also using equation (2.3) we define the operator,

$$\hat{P} = \frac{1}{2}(1 + \mathrm{i}\hat{H}), \tag{2.11}$$

projecting any 2π-periodic function f into a function which has analytical continuation from the real line $w = u$ into $\mathbb{C}^-$ as follows

$$\hat{P}f = f^- + \frac{f_0}{2}. \tag{2.12}$$

One can apply $\hat{H}$ to (2.1) to obtain the following closed expression for y,

$$\left(c^2\hat{k} - 1\right) y - \left(\frac{\hat{k}y^2}{2} + y\hat{k}y\right) = 0, \tag{2.13}$$

where $\hat{k} \equiv -\partial_u\hat{H} = \sqrt{-\nabla^2}$ and we used the following relations

$$y_u = \hat{H}\tilde{x}_u \quad \text{and} \quad \tilde{x}_u = -\hat{H}y_u, \tag{2.14}$$

which are valid for the analytic function $\tilde{z}_u(w)$ satisfying the decaying condition $\tilde{z}_u(w) \to 0$ as $v \to -\infty$. We also assume in deriving equation (2.13) from equation (2.1) that

$$\int_{-\pi}^{\pi} \eta(x,t)\mathrm{d}x = \int_{-\pi}^{\pi} y(u,t)x_u(u,t)\mathrm{d}u = 0, \tag{2.15}$$

meaning that the elevation of free surface of unperturbed fluid is set to zero. Equation (2.15) is valid at all times and reflects a conservation of the total mass of fluid.

Equation (2.13) is convenient for numerical simulation of Stokes wave because it depends on y only as detailed in Part I (Dyachenko *et al.* 2015*b*). The operator $\hat{k}$ is the multiplication operator in Fourier domain which is straightforward to evaluate numerically using Fast Fourier Transform.

In this paper it is however more convenient for analytical study to rewrite equation for Stokes wave in terms of the complex variable $\tilde{z}$. For that we apply the projector operator $\hat{P}$ (2.11) to equation (2.1) which results in

$$c^2\tilde{z}_u = -\mathrm{i}\hat{P}\left[(\tilde{z} - \bar{\tilde{z}})(1 + \tilde{z}_u)\right], \tag{2.16}$$

where $\bar{f}(u) \equiv \bar{f}$ means complex conjugation of the function $f(u)$. Note that the complex conjugation $\bar{f}(w)$ of $f(w)$ in this paper is understood as applied with the assumption that $f(w)$ is the complex-valued function of the real argument w even if w takes the complex values so that

$$\bar{f}(w) \equiv \overline{f(\bar{w})}. \tag{2.17}$$

That definition ensures the analytical continuation of $f(w)$ from the real axis $w=u$ into the complex plane of $w\in\mathbb{C}$ and similar for functions of $\zeta\in\mathbb{C}$. If the function $f(w)$ is analytic in $\mathbb{C}^-$ then $\bar f(w)$ is analytic in $\mathbb{C}^+$ as also follows from equations (2.7)-(2.9).

A numerical convergence of Padé approximation to the density of branch cut $\rho(\chi)$ was shown in Part I (Dyachenko *et al.* 2015*b*) together with the parametrization of the branch cut of Stokes wave as follows

$$\tilde z(\zeta)=\mathrm{i}y_0+\int\limits_{\chi_c}^{1}\frac{\rho(\chi')d\chi'}{\zeta-\mathrm{i}\chi'}, \tag{2.18}$$

where $y_0\equiv y(u)|_{u=\pm\pi}\in\mathbb{R}$. The density $\rho(\chi)$ is related to the jump Δ_{jump} of $\tilde z(\zeta)$ for crossing branch cut at $\zeta=\mathrm{i}\chi$ in counterclockwise direction as follows

$$\tilde\Delta_{jump}\equiv z(\zeta)|_{\zeta=\mathrm{i}\chi-0}-\tilde z(\zeta)|_{\zeta=\mathrm{i}\chi+0}=-2\pi\rho(\chi), \tag{2.19}$$

see also Part I for more details on that. We now use the parametrization (2.18) to study the Stokes wave equation (2.16). We eliminate the constant $\mathrm{i}y_0$ at $\zeta=\infty$ in (2.18) by introducing a new function

$$f(u)=\tilde z(u)-\mathrm{i}y_0=\int\limits_{\chi_c}^{1}\frac{\rho(\chi')d\chi'}{\zeta-\mathrm{i}\chi'}. \tag{2.20}$$

together with the complex conjugate

$$\bar f(u)=\int\limits_{\chi_c}^{1}\frac{\rho(\chi')d\chi'}{\zeta+i\chi'} \tag{2.21}$$

which was evaluated using the definition (2.17).

Equation (2.16) in new valuable (2.20) takes the following form

$$-ic^2f_u+\mathrm{i}y_0+2iy_0f_u+ff_u+\hat Pf-\hat P\bar f-\hat P\left[\bar ff_u\right]=0 \tag{2.22}$$

with f and $\bar f$ given by equations (2.20) and (2.21), respectively.

2.1. *Projection in ζ plane*

The projector $\hat P$ (2.11) is defined in terms of the independent variable u. Using the equation (2.22) together with the definition (2.20) suggests to switch from u into the independent variable ζ. To identify how to compute $\hat P$ in complex ζ-plane we start from the Fourier series (2.4) in variable u and make a change of variable (1.6) (assuming that $-\pi\leqslant u\leqslant\pi$ and $\zeta\in\mathbb{R}$) as follows

$$f(u)=f(\zeta)=\sum_{k=-\infty}^{\infty}f_ne^{iku}=\sum_{k=-\infty}^{\infty}f_n\exp\left[2ik\arctan\zeta\right]=\sum_{n=-\infty}^{\infty}f_k\left(\frac{\zeta-i}{\zeta+i}\right)^k(-1)^k, \tag{2.23}$$

where we abuse notation by assuming that $\tilde f(\zeta)\equiv f(u)$ and removing $\tilde{}$ sign. Equations (2.11), (2.12) and (2.23) imply that $\hat P$ removes all Fourier harmonics with positive n and

replaces zero harmonic f_0 by $f_0/2$ as follows

$$\hat{P}f(u) = \sum_{n=-\infty}^{\infty} f_k \hat{P} e^{iku} = \frac{f_0}{2} + \sum_{k=-\infty}^{-1} f_k \exp\left[ik2\arctan\zeta\right] = \frac{f_0}{2} + \sum_{n=-\infty}^{-1} f_k \left(\frac{\zeta - i}{\zeta + i}\right)^k (-1)^k. \tag{2.24}$$

Consider a particular case $f(u) = \frac{1}{\zeta - i\chi}$, $\chi \in \mathbb{R}$ and $\chi \neq 0$. We calculate f_k by the equation (2.4) and (2.23) through the change of variable (1.6) implying $du = \frac{2}{\zeta^2+1} d\zeta$ as follows

$$f_{-k} = \frac{1}{2\pi}\int_{-\pi}^{\pi} f(u) e^{iku} du = \frac{1}{2\pi}\int_{-\infty}^{\infty} \frac{1}{\zeta - i\chi}\left(\frac{\zeta - i}{\zeta + i}\right)^k (-1)^k \frac{2}{\zeta^2+1} d\zeta. \tag{2.25}$$

Assuming $k \geqslant 0$ and closing the complex integration contour in the upper half-plane of ζ we obtain that

$$f_{-k} = i\left(\frac{\chi - 1}{\chi + 1}\right)^k (-1)^k \frac{2}{-\chi^2+1}\theta(\chi) + \delta_{k,0}\frac{1}{i - i\chi}. \tag{2.26}$$

For the zero harmonic f_0 the equation (2.26) results in

$$f_0 = \frac{\mathrm{i}\,\mathrm{sign}(\chi)}{1 + \chi\,\mathrm{sign}(\chi)}, \tag{2.27}$$

where $\mathrm{sign}(\chi) = 1$ for $\chi > 0$ and $\mathrm{sign}(\chi) = -1$ for $\chi < 0$.

Using now (2.24), (2.26) and (2.27) we find that

$$\hat{P}\frac{1}{\zeta - i\chi} = \frac{-\mathrm{i}\,\mathrm{sign}(\chi)}{2[1 + \chi\,\mathrm{sign}(\chi)]} + \sum_{k=0}^{\infty}\left[i\left(\frac{\chi - 1}{\chi + 1}\right)^k (-1)^k \frac{2}{-\chi^2+1}\theta(\chi) + \delta_{k,0}\frac{1}{i - i\chi}\right] \times \left(\frac{\zeta + i}{\zeta - i}\right)^k (-1)^k = \frac{1}{\zeta - i\chi}\theta(\chi) + \frac{1}{i - i\chi}\theta(-\chi) - \frac{\mathrm{i}\,\mathrm{sign}(\chi)}{2[1 + \chi\,\mathrm{sign}(\chi)]}, \tag{2.28}$$

where $\theta(\chi) = 1$ for $\chi > 0$ and $\theta(\chi) = 0$ for $\chi < 0$.

In a similar way, for $f(\zeta) = \dfrac{1}{(\zeta - i\chi)^2}$ we find for the series (2.23) that

$$f_{-k} = \frac{1}{2\pi}\int_{-\infty}^{\infty} \frac{1}{(\zeta - i\chi)^2}\left(\frac{\zeta - i}{\zeta + i}\right)^k (-1)^k \frac{2}{\zeta^2+1} d\zeta, \quad k \geqslant 0. \tag{2.29}$$

Closing the complex integration contour in the upper half-plane of ζ one obtains from the equation (2.29) that

$$f_{-k} = i\frac{d}{d\zeta}\left(\frac{\zeta - i}{\zeta + i}\right)^k (-1)^k \frac{2}{\zeta^2+1}\theta(\chi)\bigg|_{\zeta = i\chi} + \delta_{k,0}\frac{1}{(i - i\chi)^2}, \quad k \geqslant 0 \tag{2.30}$$

and

$$f_0 = -\frac{1}{[1 + \chi\,\mathrm{sign}(\chi)]^2}. \tag{2.31}$$

Taking sum over k in the equation (2.24) using (2.30) and (2.31) and we find that

$$\hat{P}\frac{1}{(\zeta-i\chi)^2}=\frac{1}{(\zeta-i\chi)^2}\theta(\chi)+\frac{1}{(i-i\chi)^2}\theta(-\chi)+\frac{1}{2[1+\chi\,\mathrm{sign}(\chi)]^2}. \tag{2.32}$$

2.2. *Integral representation of the equation for Stokes wave*

Using the equations (2.20), (2.28) and (2.32) we obtain the following projections in terms of $\rho(\chi)$:

$$\hat{P}f=\int\limits_{\chi_c}^{1}\frac{\rho(\chi)d\chi}{\zeta-i\chi}-\int\limits_{\chi_c}^{1}\frac{\mathrm{i}\rho(\chi)d\chi}{2(1+\chi)},\qquad \hat{P}\bar{f}=-\int\limits_{\chi_c}^{1}\frac{\mathrm{i}\rho(\chi)d\chi}{2(1+\chi)}. \tag{2.33}$$

We now find $\hat{P}\left[\bar{f}f_u\right]$ used in (2.22). Equation (1.6) results in the following expression

$$\bar{f}f_u=\frac{\zeta^2+1}{2}\bar{f}f_\zeta=-\frac{\zeta^2+1}{2}\int\limits_{\chi_c}^{1}\int\limits_{\chi_c}^{1}\frac{\rho(\chi')\rho(\chi'')d\chi'd\chi''}{(\zeta+i\chi')(\zeta-i\chi'')^2} \tag{2.34}$$

We perform the partial fraction decomposition of the integrand of (2.34) as follows

$$\begin{aligned}-\frac{\zeta^2+1}{2(\zeta+i\chi')(\zeta-i\chi'')^2}=\frac{1}{\zeta+i\chi'}\frac{1-\chi'^2}{2(\chi'+\chi'')^2}+\frac{1}{\zeta-i\chi''}\frac{-1-2\chi'\chi''-\chi''^2}{2(\chi'+\chi'')^2}\\ +\frac{1}{(\zeta-i\chi'')^2}\frac{i(1-\chi''^2)}{2(\chi'+\chi'')}.\end{aligned} \tag{2.35}$$

and apply the projector $\hat{P}$ to (2.35) which gives with the use of (2.28) and (2.32) the following expression:

$$\begin{aligned}\hat{P}\left[\bar{f}f_u\right]=\int\limits_{\chi_c}^{1}\int\limits_{\chi_c}^{1}\left[\frac{1}{i+i\chi'}\frac{1-\chi'^2}{4(\chi'+\chi'')^2}+\left(\frac{1}{\zeta-i\chi''}-\frac{\mathrm{i}}{2(1+\chi'')}\right)\frac{-1-2\chi'\chi''-\chi''^2}{2(\chi'+\chi'')^2}\right.\\ \left.+\left(\frac{1}{(\zeta-i\chi'')^2}+\frac{1}{2(1+\chi'')^2}\right)\frac{i(1-\chi''^2)}{2(\chi'+\chi'')}\right]\rho(\chi')\rho(\chi'')d\chi'd\chi''.\end{aligned} \tag{2.36}$$

The other nonlinear term in equation (2.22) has the following integral form

$$ff_u=\frac{1}{2}(1+\zeta^2)ff_\zeta=-\frac{1}{2}(1+\zeta^2)\int\limits_{\chi_c}^{1}\frac{\rho(\chi')d\chi'}{(\zeta-i\chi')}\int\limits_{\chi_c}^{1}\frac{\rho(\chi'')d\chi''}{(\zeta-i\chi'')^2}. \tag{2.37}$$

The constant y_0 is determined from equation (2.15) as follows

$$\int\limits_{-\pi}^{\pi}y(1+\tilde{x}_u)du=\int\limits_{-\infty}^{\infty}\left[y_0+\frac{(f-\bar{f})}{2\mathrm{i}}\right]\left[1+\frac{(1+\zeta^2)}{4}(f_\zeta+\bar{f}_\zeta)\right]\frac{2d\zeta}{1+\zeta^2}=0, \tag{2.38}$$

which results using (2.20) in the following equation

$$y_0=-\int\limits_{\chi_c}^{1}\int\limits_{\chi_c}^{1}\frac{\rho(\chi')\rho(\chi'')d\chi'd\chi''}{2(\chi'+\chi'')^2}-\int\limits_{\chi_c}^{1}\frac{\rho(\chi')d\chi'}{1+\chi'}. \tag{2.39}$$

Equation (2.39) allows to find y_0 from a given $\rho(\chi)$. This equation also provides a convenient tool to estimate the accuracy of recovering $\rho(\chi)$ by Padé approximation. For

that one compares the numerical value of y_0 obtained from the Stokes solution in Part I (Dyachenko *et al.* 2015*b*) with the result of the direct numerical calculation of right-hand side (r.h.s.) of the equation (2.39) with $\rho(\chi)$ obtained from Padé approximation in Part I (all these numerical values are given in the electronic attachment in Part I).

Requiring that equations (2.20)-(2.22), (2.33), (2.36), (2.37) and (2.39) are satisfied for $-\infty < \zeta < \infty$ we obtain a closed system of equations to find the density $\rho(\chi)$ along the branch cut for each c. That system has a form of nonlinear integral equation for the unknown function $\rho(\chi)$. Taking the limit $\zeta \to \infty$ in that system results in the following compact expression

$$\frac{c^2}{2c_0^2}\int\limits_{\chi_c}^{1}\rho(\chi')d\chi' + 2\left[-\int\limits_{\chi_c}^{1}\int\limits_{\chi_c}^{1}\frac{\rho(\chi')\rho(\chi'')d\chi'd\chi''}{2(\chi'+\chi'')^2} - \int\limits_{\chi_c}^{1}\frac{\rho(\chi')d\chi'}{1+\chi'}\right]$$
$$\times\left[1-\frac{1}{2}\int\limits_{\chi_c}^{1}\rho(\chi''')d\chi'''\right] + \int\limits_{\chi_c}^{1}\frac{\rho(\chi')d\chi'}{1+\chi'} + \int\limits_{\chi_c}^{1}\int\limits_{\chi_c}^{1}\frac{(1-\chi')\rho(\chi')\rho(\chi'')d\chi'd\chi''}{2(\chi'+\chi'')^2} = 0. \quad (2.40)$$

To solve the system (2.20)-(2.22), (2.33), (2.36), (2.37) and (2.39) numerically one can approximate all integrals by any desired numerical quadrature evaluated at the discrete set of points $-\infty < \zeta = \zeta_j < \infty,\ j = 1, 2, \dots N$. Then one obtains the nonlinear algebraic system of equations to find $\rho(\chi)$. That system is overdetermined provided the number of points N in ζ is chosen to exceed the number of points (parameters) in the numerical quadrature for $\rho(\chi)$. Then the nonlinear algebraic system can be solved in least square sense (by minimizing the sum of squares of the left-hand side (l.h.s.) of the equation (2.22) taken over $\zeta_j,\ j = 1, 2, , \dots N$). The difficulty in that numerical scheme is that the lower limit of integration, χ_c, is unknown thus its approximate value creates small oscillations of $\rho(\chi)$ near the true value of χ_c. One way to overcome that difficulty is to repeat that numerical procedure iteratively aiming to suppress these oscillations.

Second way is to use the expansion of $z(\zeta)$ in powers of $(\zeta - \mathrm{i}\chi_c)^{n/2},\ n = 1, 2, \dots$ at $\zeta = i\chi_c$ to find an additional condition for finding χ_c. We use the expansion

$$f(\zeta) = \sum_{j=0}^{\infty} \mathrm{i}e^{\mathrm{i}j\pi/4}a_j(\zeta - \mathrm{i}\chi_c)^{j/2}, \quad (2.41)$$

where a_j are real constants. The complex conjugate of equation (2.41),

$$\bar{f}(\zeta) = \sum_{j=0}^{\infty} -ie^{-ij\pi/4}a_j(\zeta + i\chi_c)^{j/2}, \quad (2.42)$$

is the analytic function at $\zeta = i\chi_c$. Plugging in (2.41), (2.42) into the equation (2.22) and collecting the terms with $(\zeta - i\chi_c)^{-1/2}$ one obtains that

$$a_1\frac{\mathrm{i}e^{\mathrm{i}\pi/4}(1-\chi_c^2)}{4(\zeta - \mathrm{i}\chi_c)^{1/2}}\left[-\mathrm{i}c^2 + 2\mathrm{i}y_0 + f(\mathrm{i}\chi_c) - \bar{f}(\mathrm{i}\chi_c)\right] = 0 \quad (2.43)$$

which implies

$$-\mathrm{i}c^2 + 2\mathrm{i}y_0 + f(\mathrm{i}\chi_c) - \bar{f}(\mathrm{i}\chi_c) = 0, \quad (2.44)$$

where $f(\mathrm{i}\chi_c) = \mathrm{i}a_0$ and $\bar{f}(\mathrm{i}\chi_c)$ is given by equation (2.42) with $\zeta = \mathrm{i}\chi_c$. Equation (2.44) provides a desired additional condition to find χ_c. Then the numerical iteration procedure is the following: at each iteration (for each value of χ_c) one solves the equations (2.20)-(2.22), (2.33), (2.36), (2.37) and (2.39) numerically to approximate $\rho(\chi)$. Then l.h.s. of

equation (2.44) is calculated using equations (2.20),(2.21) and (2.39). That l.h.s. is used in Newton iterations over χ_c aiming to satisfy equation (2.44). The practical realization of that numerical scheme is beyond the scope of this paper.

3. Alternative form for the equation of Stokes wave

Equation for Stokes wave can be written in a form which is alternative to equation (2.1) as follows

$$y = -\frac{\mathrm{i}}{2}(\tilde{z} - \bar{\tilde{z}}) = -\frac{\mathrm{i}}{2}(z - \bar{z}) = \frac{c^2}{2}\left(1 - \frac{1}{|z_u|^2}\right). \tag{3.1}$$

Appendix A shows the equivalence of both forms of equations (2.1) and (3.1) for Stokes wave. Also Appendix B discussed differences in derivation of equations (2.1) and (3.1) from basic equations of the potential flow of ideal fluid with free surface.

Transforming equation (3.1) into the variable ζ (1.6) results in

$$\tilde{z} - \bar{\tilde{z}} = \mathrm{i}c^2\left(1 - \frac{4}{(1+\zeta^2)^2|z_\zeta|^2}\right). \tag{3.2}$$

Solving equation (3.1) for z_u one obtains that

$$z_u = \frac{c^2}{\bar{z}_u[\mathrm{i}(z - \bar{z}) + c^2]} \tag{3.3}$$

which is the nonlinear ODE provided $\bar{z}_u$ is known. In a similar way, equation (3.2) results in

$$z_\zeta = \frac{4}{(1+\zeta^2)^2}\frac{c^2}{\bar{z}_\zeta[\mathrm{i}(z - \bar{z}) + c^2]}. \tag{3.4}$$

Equations (3.3) and (3.4) can be considered as ODEs for $z(u)$ and $z(\zeta)$, respectively, provided $\bar{z}$ is the known function. Then solving ODE provides a convenient tool to study the analytical properties of Stokes wave in different sheets of Riemann surface of z.

4. Asymptotic of Stokes wave at $Im(w) \to +\infty$ and jump at branch cut

An asymptotical solution of Stokes at $Im(w) \to +\infty$ is obtained from equation (3.3) as follows. Equation (2.9) implies the exponential convergence $\propto e^{\mathrm{i}w}$ of $\tilde{z}(w)$ to zero Fourier harmonic, $\tilde{z}(w) \to \mathrm{i}y_0$ for $Im(w) \to -\infty$. Respectively, $\bar{\tilde{z}}(w)$ converges exponentially to $-\mathrm{i}y_0$ for $Im(w) \to \infty$. Then $\bar{z}_u$ and $\bar{z}$ in equation (3.3) can be replaced by 1 and $-\mathrm{i}y_0$, respectively in that limit resulting in

$$1 + \tilde{z}_u = \frac{c^2}{\mathrm{i}(\tilde{z} + \mathrm{i}y_0) + c^2}, \qquad Im(w) \to \infty. \tag{4.1}$$

Integrating equation (4.1) in upper right quadrant $w \in \mathbb{C}^+,\ Re(w) > 0$ for $v \gg 1$, one obtains that

$$\tilde{z}(w) - \mathrm{i}c^2 \ln\left[\tilde{z}(w) + \mathrm{i}y_0\right] = -w + c_+, \tag{4.2}$$

where c_+ is the constant. A similar integration in upper right quadrant $w \in \mathbb{C}^+,\ Re(w) < 0$, for $v \gg 1$ results in

$$\tilde{z}(w) - \mathrm{i}c^2 \ln\left[\tilde{z}(w) + \mathrm{i}y_0\right] = -w + c_-, \tag{4.3}$$

where c_- is the constant.

Taking $w = \pi + \mathrm{i}v$ in equation (4.2) and $w = -\pi + \mathrm{i}v$ in equation (4.3) together with

the periodicity condition $\tilde{z}(\pi + \mathrm{i}v) = \tilde{z}(-\pi + \mathrm{i}v)$ result in the condition for constants c_+ and c_- as follows

$$c_- - c_+ = -2\pi. \tag{4.4}$$

Exponents of equations (4.2) and (4.3) are similar to the Lambert W-function. Solving these equations in the limit $v \to \infty$ (see e.g. Refs. Dyachenko *et al.* (2013); Lushnikov *et al.* (2013) for details on a similar technique) one obtains that

$$\tilde{z}(w) = -w + c_\pm + \mathrm{i}c^2 \ln\left[-w + c_\pm + \mathrm{i}y_0\right] - \frac{c^4 \ln\left[-w + c_\pm + \mathrm{i}y_0\right]}{-w + c_\pm + \mathrm{i}y_0} + O\left(\frac{\ln\left[-w + c_\pm + \mathrm{i}y_0\right]}{-w + c_\pm + \mathrm{i}y_0}\right)^2, \tag{4.5}$$

where a use of c_+ and c_- assumes that $Re(w) > 0$ and $Re(w) < 0$, respectively. If equation (3.3) is used instead of the reduced equation (4.1) in derivation of equation (4.5), then an additional exponentially small error term $O(e^{-v}/v)$ appears in r.h.s. of (4.5).

One concludes from equation (4.5) that $z(w)$ has a complex singularity at $z = \infty$ which involves logarithms with the infinite number of sheets of Riemann surface. Full analysis of that singularity requires to study next order terms in equation (4.5) which is beyond the scope of this paper.

Taking an additional limit $w = \mathrm{i}v \pm \epsilon$, $\epsilon > 0$, $\epsilon \to 0$ in equation (4.1), using the condition (4.4) and expanding in $v \gg 1$, one obtains the jump at branch cut

$$z(\mathrm{i}v - 0) - z(\mathrm{i}v + 0) = -2\pi + \frac{2\pi c^2}{v} + O(v^{-2}), \tag{4.6}$$

where branch cut $v \in [\mathrm{i}v_c, \mathrm{i}\infty]$ is crossed in counterclockwise direction.

According to equation (2.19), the jump (4.6) is related to the density $\rho(\chi)$ (2.18) as follows

$$\rho(\chi)|_{\chi=\tanh(v/2)} = 1 - \frac{c^2}{v} + O(v^{-2}), \quad v \gg 1. \tag{4.7}$$

For $v \gg 1$, one obtains from equation (1.6) that $1 - \chi \ll 1$ and $v = -\ln\left(\frac{1-\chi}{2}\right) + O(1-\chi)$. Then the density (4.7) takes the following form

$$\rho(\chi) = 1 + \frac{c^2}{\ln\left(\frac{1-\chi}{2}\right)} + O\left(\frac{1}{\ln^2(1-\chi)}\right). \tag{4.8}$$

Equation (4.8) implies a unit value

$$\rho(1) = 1 \tag{4.9}$$

and the divergence of the derivative

$$\frac{d\rho(\chi)}{d\chi} \simeq \frac{c^2}{(1-\chi)\ln^2\left(\frac{1-\chi}{2}\right)} \to \infty \text{ for } \chi \to 1. \tag{4.10}$$

5. Numerical procedure to analyze the structure of sheets of Riemann surface for Stokes wave by ODE integration

We use Padé approximants of Stokes wave found in Part I (Dyachenko *et al.* 2015*b*) and provided both in electronic attachment of Dyachenko *et al.* (2015*b*) and through the

web link Dyachenko *et al.* (2015*a*) in the following form

$$z_{pade}(u) \equiv u + \mathrm{i}y_0 + \sum_{n=1}^{N} \frac{\gamma_n}{\tan(u/2) - \mathrm{i}\chi_n}, \tag{5.1}$$

with the numerical values of y_0, the pole positions χ_n and the complex residues γ_n ($n = 1, \dots, N$) given there. These data of Padé approximation allow to recover the Stokes wave at the real axis $w = u$ (and similar at $\zeta = Re(\zeta)$ in the complex ζ-plane) with the relative accuracy of at least 10^{-26} (for the vast majority of numerical cases the actual accuracy is even higher by several orders of magnitude).

Analytical continuation of the Padé approximant (5.1) from u to $w \in \mathbb{C}$ is given by the straightforward replacing of u by w. That analytical continuation is accurate for $w \in \mathbb{C}^-$ but looses precision for $w \in \mathbb{C}^+$ in the neighbourhood of the branch cut $w \in [\mathrm{i}v_c, \mathrm{i}\infty)$ where the discrete sum (5.1) fails to approximate the continuous paramterization (2.18) of the branch cut. Thus a significant loss of precision compare to 10^{-26} occurs only if the distance from ζ to the branch cut is smaller or comparable with the distance between neighbouring values of χ_n in equation (5.1).

At the first step of our investigation, ODE (3.4) was solved numerically to find the approximation $z_{ODE}(\zeta)$ for $z(\zeta)$ with $\zeta \in \mathbb{C}^+$ in the first and the second sheet of Riemann surface using the approximants (5.1) for $\bar{z}$ and $\bar{z}_\zeta$ in ODE (3.4). Here the first (physical) sheet of Riemann surface corresponds to $z(\zeta)$ with fluid occupying $\zeta \in \mathbb{C}^-$. The second (non-physical) sheet is reached when the branch cut $\zeta \in [\mathrm{i}\chi_c, \mathrm{i}]$ (or equivalently $w \in [\mathrm{i}v_c, \mathrm{i}\infty)$) is crossed from the first sheet. That ODE was solved with initial conditions at real line $\zeta = Re(\zeta)$ and integrating along different contours in $\zeta \in \mathbb{C}^+$. A high precision of at least 10^{-30} was achieved in ODE solver to avoid any significant additional loss of precision compare with 10^{-26} precision of equation (5.1). That ODE solution used $\bar{z}_{pade}$ and $(\bar{z}_{pade})_\zeta$ which through the complex conjugation corresponds to the approximants (5.1) in $\zeta \in \mathbb{C}^-$ thus avoiding any loss of precision compare with 10^{-26}. The ODE solution in the second sheet is obtained when integrating contour crossed the branch cut $[\mathrm{i}\chi_c, \mathrm{i}]$. The second subsequent crossing of that branch cut returns $z_{ODE}(\zeta)$ to the first sheet confirming square-root branch point at $\zeta = \mathrm{i}\chi_c$. In other words, it was found that ODE integration along any closed contour in $\zeta \in \mathbb{C}^+$ with double crossing of the branch cut always returns the solution to the original one. The second step of our investigation was to find $z(\zeta)$ by integrating ODE (3.4) in the second sheet with $\zeta \in \mathbb{C}^-$ using the complex conjugate of $z_{ODE}(\zeta)$, $\zeta \in \mathbb{C}^+$ found at previous step to approximate for $\bar{z}, \bar{z}_\zeta$. Initial condition at that step was at the real line $\zeta = Re(\zeta)$ with $z(\zeta)$ obtained at the step one for the second sheet.

The second step reveals a new square-root singularity at $\zeta = -\mathrm{i}\chi_c$ in the second sheet. Crossing of the branch cut $[-\mathrm{i}\chi_c, -\mathrm{i}]$ (corresponds to that new branch point $\zeta = -\mathrm{i}\chi_c$) allows to go into the third sheet of Riemann surface. At that crossing one has to simultaneously cross from the first to the second sheets for $\bar{z}, \bar{z}_\zeta$ which again are the complex conjugate of $z_{ODE}(\zeta)$, $\zeta \in \mathbb{C}^+$ found at previous step. It was found that the third sheet has branch points both at $\zeta = \mathrm{i}\chi_c$ and $\zeta = -\mathrm{i}\chi_c$. In a similar way to previous steps, at the step three one crosses the branch cut $[\mathrm{i}\chi_c, \mathrm{i}]$ to go into the fourth sheet of Riemann surface which found to has branch points both at $\zeta = \mathrm{i}\chi_c$ and $\zeta = -\mathrm{i}\chi_c$. At the step four one crosses the branch cut $[-\mathrm{i}\chi_c, -\mathrm{i}]$ to go into the firth sheet of Riemann surface which again has branch points both at $\zeta = \mathrm{i}\chi_c$ and $\zeta = -\mathrm{i}\chi_c$ etc. At each sheet, $\bar{z}, \bar{z}_\zeta$ used in integration of ODE (3.4) is behind by one to the current sheet, i.e. values of $\bar{z}, \bar{z}_\zeta$ from the first, second, third etc. sheets are used for ODE integration in the second, third, fourth etc. sheets, respectively. After exploring several hundreds of sheets

for different values of χ_c, one concludes that the number of sheets is infinite. In next section this conjecture is strengthened by the analysis of expansions at $\zeta = \pm\chi_c$ in these multiple sheets.

By-product of ODE integration of this section is that one can also calculate the jump $-2\pi\rho(\chi)$ (see equation (2.18)) at the branch cut of the first sheet with the high precision. E.g. one can start ODE integration at $\zeta = 0$ in the first sheet and integrate until reaching a small neighborhood of $\zeta = \mathrm{i}\chi_c$ without crossing the branch cut $\zeta \in [\mathrm{i}\chi_c, \mathrm{i}]$. After that one can integrate ODE independently along two line segments $\zeta = [\pm\epsilon + \mathrm{i}\chi_c, \pm\epsilon + \mathrm{i}]$, $\epsilon \to 0$ and calculate difference between these two integrations recovering $\rho(\chi)$ with the precision of our simulations $\sim 10^{-26}$. Comparison of that high precision $\rho(\chi)$ with the numerical approximation of $\rho(\chi)$ obtained in Part I from the continuous limit of Padé approximation confirmed the numerical error order estimates of Section 4.2 of Part I. Also we found that equations (4.6)-(4.10) are also in excellent agreement with the numerical values of $\rho(\chi)$ confirming the asymptotical analysis of Section 4.

Note that it was assumed throughout this Section that any crossing by the ODE integration contour of both $[\mathrm{i}, \mathrm{i}\infty]$ and $[-\mathrm{i}, -\mathrm{i}\infty]$ is avoided. Such crossing would be harmless in the first sheet because of 2π-periodicity of $\tilde{z}(w)$. However, starting from the second sheet, $\tilde{z}(w)$ is generally non-periodic in w. Thus the branch cuts $[\mathrm{i}, \mathrm{i}\infty]$ and $[-\mathrm{i}, -\mathrm{i}\infty]$ cannot be ignored any more as was the case for the first sheet case discussed in the Introduction.

6. Series expansions at $\zeta = \pm i\chi_c$ and structure of Riemann surface for Stokes wave

The equation (3.1) together with the definition (2.17) shows that singularities at $\zeta = \pm i\chi_c$ are coupled through complex conjugation. We found in Part I (Dyachenko *et al.* 2015*b*) that there is only one singularity (a square-root branch point) in the first (physical) sheet of Riemann surface which corresponds to the finite complex w plane. In addition, there is a singularity at $\zeta = \mathrm{i}$ which is the complex infinity $w = \mathrm{i}\infty$ and is discussed in Section 4. Following Part I we chose the line segment $[\mathrm{i}\chi_c, \mathrm{i}]$ as the branch cut connecting these two singularities in the first sheet of Riemann surface as sketched on the left panel of Figure 1. Singularity at $\zeta = -\mathrm{i}\chi_c$ is not allowed in the first sheet because z is analytic in the fluid domain $w \in \mathbb{C}^-$.

Consider the expansions in lth sheet of Riemann surface

$$z_{l,+}(\zeta) = \sum_{j=0}^{\infty} \mathrm{i} e^{\mathrm{i}j\pi/4} a_{+,l,j} (\zeta - \mathrm{i}\chi_c)^{j/2}, \quad l = 1, 2, \ldots, \tag{6.1}$$

and

$$z_{l,-}(\zeta) = \sum_{j=0}^{\infty} \mathrm{i} e^{-\mathrm{i}j\pi/4} a_{-,l,j} (\zeta + \mathrm{i}\chi_c)^{j/2}, \quad l = 1, 2, \ldots, \tag{6.2}$$

where subscripts "+" and "-" mean expansions at $\zeta = i\chi_c$ and $\zeta = -i\chi_c$, respectively. Here branch cuts of $(\zeta - \mathrm{i}\chi_c)^{1/2}$ and $(\zeta + \mathrm{i}\chi_c)^{1/2}$ are assumed to extend from $\zeta = \mathrm{i}\chi_c$ upwards and from $\zeta = -\mathrm{i}\chi_c$ downwards, respectively. Often a location of branch cut of square root is taken on the negative real axis of the argument. To use that standard agreement about a location of branch cut, one can replace $(\zeta - \mathrm{i}\chi_c)^{j/2}$ and $(\zeta + \mathrm{i}\chi_c)^{j/2}$ in equations (6.1) and (6.2) by $(-\mathrm{i})^{j/2}(\mathrm{i}\zeta + \chi_c)^{j/2}$ and $\mathrm{i}^{j/2}(-\mathrm{i}\zeta + \chi_c)^{j/2}$, respectively.

We enumerate sheets of Riemann surface corresponding to the branch points $\zeta = \pm\mathrm{i}\chi_c$ as follows. A crossing of branch cut $[\mathrm{i}\chi_c, \mathrm{i}]$ in the counterclockwise direction means going

from $l=2n-1$th sheet of Riemann surface to $l=2n$th sheet with $n=1,2,\ldots$. Case $l=1$ corresponds to the physical sheet of Riemann surface. Similarly, crossing a branch cut $[-\mathrm{i}\chi_c,-\mathrm{i}]$ in the counterclockwise direction means going from $l=2n$th sheet of Riemann surface to $l=2n+1$ sheet with $n=1,2,\ldots$. Plugging in expansions (6.1) and (6.2) into equation (3.1) and collecting terms of the same order of $(\zeta\pm\mathrm{i}\chi_c)^{j/2}$ result in the following relations

$$\begin{aligned}
&a_{-,2n,1}=0,\\
&a_{-,2n,2}=\frac{-2}{1-{\chi_c}^2},\\
&a_{-,2n,3}=\frac{16c^2}{3\left(1-\chi_c^2\right)^2 a_{+,2n-1,1}(c^2-a_{+,2n-1,0}-a_{-,2n,0})},\\
&a_{-,2n,4}=\frac{2\chi_c}{(1-{\chi_c}^2)^2}+\frac{4c^2}{(1-{\chi_c}^2)^2(c^2-a_{+,2n-1,0}-a_{-,2n,0})^2}\\
&\qquad-\frac{8c^2[2+(-1+\chi_c^2)a_{+,2n-1,2}]}{(1-{\chi_c}^2)^3a_{+,2n-1,1}^2(c^2-a_{+,2n-1,0}-a_{-,2n,0})},\\
&\ldots
\end{aligned}\tag{6.3}$$

for $n\geqslant 1$ and

$$\begin{aligned}
&a_{+,2n+1,1}=-\frac{16c^2}{3\left(1-{\chi_c}^2\right)^2 a_{-,2n,3}(c^2-a_{-,2n,0}+a_{+,2n+1,0})},\\
&a_{+,2n+1,2}=\frac{2}{1-{\chi_c}^2}+\frac{128c^4}{9(1-{\chi_c}^2)^4a_{-,2n,3}^2(c^2-a_{-,2n,0}-a_{+,2n+1,0})^3}\\
&\qquad+\frac{32c^2[-2\chi_c+(1-\chi_c^2)^2a_{-,2n,4}]}{9(1-{\chi_c}^2)^4a_{-,2n,3}^2(c^2-a_{-,2n,0}-a_{+,2n+1,0})},\\
&a_{+,2n+1,3}=\ldots,\\
&\ldots
\end{aligned}\tag{6.4}$$

for $n\geqslant 1$.

One cannot take $n=0$ in equation (6.4) which corresponds to $l=1$ (the physical sheet of Riemann surface). This special case has to be considered separately because in the physical sheet there is no singularity at $\zeta=-i\chi_c$ (no singularity inside fluid domain). It implies that

$$a_{-,1,2j+1}=0\quad\text{for}\quad j=0,1,2,\ldots\tag{6.5}$$

Solving (6.1), (6.2) and (3.1) for $l=1$ with the series expansion at $\zeta=-i\chi_c$ subject to

the condition (6.5) results in the following expressions

$$
\begin{aligned}
a_{+,1,0} &= c^2 - a_{-,1,0},\\
a_{+,1,1} &= \frac{-2^{3/2}c}{(1-{\chi_c}^2)^{1/2}\left[(2+(1-\chi_c^2)a_{-,1,2})\right]^{1/2}},\\
a_{+,1,2} &= \frac{4}{3\,(1-{\chi_c}^2)} - \frac{a_{-,1,2}}{3},\\
a_{+,1,3} &= -\frac{\left[2+(1-\chi_c^2)a_{-,1,2})\right]^{5/2}}{2^{1/2}18c\,(1-{\chi_c}^2)^{3/2}}\\
&\quad + \frac{2^{1/2}c\left[2\chi_c - 2\chi_c(-1+\chi_c^2)a_{-,1,2} + (-1+\chi_c^2)^2 a_{-,1,4}\right]}{(1-{\chi_c}^2)^{3/2}\left[2+(1-\chi_c^2)a_{-,1,2})\right]^{3/2}},\\
a_{+,1,4} &= \dots,\\
&\dots
\end{aligned}
\tag{6.6}
$$

Expressions (6.6) are uniquely determined by values of c, χ_c and $a_{-,1,2j}$, $j = 0, 1, 2, \dots$, where all expressions under square roots are positive and the principle branch of all square roots is assumed. In contrast, expressions (6.3) and (6.4) are not the unique solutions of the equations (6.1), (6.2) and (3.1). In addition to the solution (6.3), one can obtain two more spurious solutions for $a_{-,2n,j}$. However, these spurious solutions do not correspond to Stokes wave. One spurious solution has $a_{-,2n,2j+1} = 0 \quad \text{for} \quad j = 1, 2, \dots$, i.e. it does not have a singularity at $\zeta = -i\chi_c$. Second spurious solution has either a radius of convergence well below χ_c or even the zero radius of convergence. Both solutions are spurious because they cannot have the same value as in the region of overlap of the disks of convergence of both expansions (6.1) and (6.2). After spurious solutions for $a_{-,2n,j}$ are discarded, the solution (6.4) $a_{+,2n+1,j}$ also turns to be uniquely defined. Another peculiar property of the solution (6.3) is that $a_{-,2n,1} = 0$ while $a_{+,2n+1,1} \neq 0$ as given by the solution (6.4).

R.h.s. of equation (6.4) provides the explicit expressions for the coefficients $a_{+,2n+1,j}$, $j = 1, 2, , \dots$, for $2n+1$th sheet of Riemann surface through the coefficients $a_{-,2n,j_1}$, $0 \leqslant j_1 \leqslant j+2$ at $2n$th sheet. The only coefficient which remains unknown is the zeroth coefficient $a_{+,2n+1,0}$ for each $n \geqslant 1$. In a similar way, r.h.s. of the equation (6.3) provides the explicit expressions for the coefficients $a_{-,2n,j}$ $j = 1, 2, , \dots$, for $2n$th sheet of Riemann surface through the coefficients $a_{+,2n-1,j_1}$, $0 \leqslant j_1 \leqslant j-2$, $j = 1, 2, , \dots$, at $2n-1$th sheet. The only coefficient which remains unknown is the zeroth coefficient $a_{-,2n,0}$ for each $n \geqslant 1$.

The explicit expressions for $a_{+,2n+1,j}$ and $a_{-,2n,j}$ turn cumbersome with the increase of j beyond values shown explicitly in equations (6.3) and (6.4). The explicit expression $a_{+,2n+1,j}$ and $a_{-,2n,j}$ were obtained with the help of symbolic computations in Mathematica software. These expressions were used to calculate values of all coefficients $a_{+,2n+1,j}$ and $a_{-,2n,j}$ for $j \geqslant 1$ numerically with any desired precision (typically we used quadruple (quad) precision with 32 digits accuracy and took into account all j in the range $1 \geqslant j \geqslant 200$). The remaining coefficients $a_{-,2n,0}$ and $a_{+,2n+1,0}$ for each $n \geqslant 1$ as well as the numerical value of χ_c were determined by a numerical procedure which is described below in Sections 6.1 and 6.2.

Values of $a_{+,2n+2,j}$ and $a_{-,2n+1,j}$ are obtained from $a_{+,2n+1,j}$, and $a_{-,2n,j}$ by the

following relations

$$\begin{aligned} a_{+,2n+2,j} &= (-1)^j a_{+,2n+1,j}, \quad n = 0, 1, 2, \dots, \\ a_{-,2n+1,j} &= (-1)^j a_{-,2n,j}, \quad n = 1, 2, \dots, \end{aligned} \tag{6.7}$$

which immediately follows from the condition at the crossing of branch cuts.

6.1. *Finding of χ_c, from matching the series expansions at $\zeta = \pm i\chi_c$ in the first sheet*

Equations (6.6) determine values of $a_{+,1,j}$, $j = 0, 1, 2, \dots$ from $a_{-,1,2j}$, $j = 0, 1, 2, \dots$ thus relating the series expansions at $\zeta = -\mathrm{i}\chi_c$ and $\zeta = \mathrm{i}\chi_c$ at the first sheet. The series at $\zeta = -\mathrm{i}\chi_c$ is given by equation (6.2) with $l = 1$ together with the condition (6.5). Thus that series contains only integer powers of $\zeta + \mathrm{i}\chi_c$. The disk of convergence $|\zeta + \mathrm{i}\chi_c| < r$ of that series is determined by the branch point at $\zeta = \mathrm{i}\chi_c$ which implies that the radius of convergence is $r = 2\chi_c$. The series at $\zeta = \mathrm{i}\chi_c$ at the first sheet is given by equations (6.1), (6.6) and contains both integer and half-integer powers of $\zeta - \mathrm{i}\chi_c$. The disk of convergence $|\zeta - \mathrm{i}\chi_c| < r$ is determined by the branch point at $\zeta = -\mathrm{i}\chi_c$ of the second sheet. Thus the radius of convergence is also $r = 2\chi_c$. In other words, the radius of convergence of the series (6.1), (6.6) in the physical sheet is determined by the singularity in the second (non-physical sheet).

Numerical values of the coefficients $a_{-,1,2j}$, $j = 0, 1, 2, \dots$ are immediately obtained by the differentiation of the Padé approximants of Part I for each numerical value of H/λ. Accuracy of that approximation of the coefficients $a_{-,1,2j}$ is checked by plugging these numerical values into the series (6.2) with $l = 1$ and using (6.5). For numerical evaluation that series is truncated to a finite sum

$$z_{1,-,sum}(\zeta) = \sum_{j=0}^{j_{max}} \mathrm{i} e^{-\mathrm{i}j\pi/4} a_{-,1,j} (\zeta + \mathrm{i}\chi_c)^{j/2} = \sum_{j=0}^{j_{max}/2} \mathrm{i} e^{-\mathrm{i}j\pi/2} a_{-,1,2j} (\zeta + \mathrm{i}\chi_c)^{j}, \tag{6.8}$$

where j_{max} is chosen sufficiently large to match the numerical precision of Padé approximants. It is convenient to evaluate that sum at $\zeta = 0$ which is well inside the disk of convergence $|\zeta + \mathrm{i}\chi_c| < 2\chi_c$. It was found that $j_{max} = 200$ at $\zeta = 0$ is well sufficient to reach a numerical precision about quad precision $\sim 10^{-32}$ of simulations of Part I. That numerical value of j_{max} (sufficient to reach quad precision) is only weakly dependent on H/λ. To understand that weak dependence one can note that $|\zeta + \mathrm{i}\chi_c|_{\zeta=0} = \chi_c$ which is one-half of the radius of convergence of the series (6.2). The asymptotics of the terms of the series (6.2) for large j is determined by the radius of convergence as follows $|a_{-,1,2j}/a_{-,1,2j+2}| \simeq 2\chi_c$. Then the truncation of the series (6.2) by the finite sum (6.8) with $j_{max} = 200$ gives the error $\sim a_{-,1,j_{max}} \chi_c^{j_{max}/2} \sim 2^{-j_{max}/2} \sim 10^{-30}$ in comparison with Padé approximation of Stokes wave at $\zeta = 0$.

It worth to note here that the number of derivatives $j_{max}/2 = 100$ which was realiably recovered above from Padé approximation is really large which demonstrates the highly superior efficiency of Padé approximation compare with Fourier series. E.g., if instead Padé approximation of Stokes wave, one uses the Fourier series representation of Stokes wave, then the number of derivatives calculated from that series with a high numerical precision would be limited to just a few (or 10-20 derivatives if the relative error ~ 1 in derivatives is allowed).

To obtain numerical values of $a_{+,1,j}$, $j = 0, 1, 2, \dots$ from equations (6.6) one also has to know the numerical value of χ_c. Part I described a numerical procedure to recover χ_c with the accuracy $\sim 10^{-10}$ which is significantly below the accuracy $\lesssim 10^{-26}$ of numerical Stokes solution itself and its Padé approximation. In this paper to greatly improve that

precision of χ_c one sets a condition that χ_c is chosen in such a way to allow the series (6.1) to recover the value of $z(0)$ with the accuracy better than $\sim 10^{-26}$.

Similar to equation (6.8), the series (6.1) is truncated to a finite sum

$$z_{1,+,sum}(\zeta) = \sum_{j=0}^{j_{max}} \mathrm{i} e^{\mathrm{i}j\pi/4} a_{+,1,j} (\zeta - \mathrm{i}\chi_c)^{j/2}, \tag{6.9}$$

where we again choose that $j_{max} = 200$ which is well enough to match quad precision $\sim 10^{-32}$. Contrary to equation (6.8), the sum (6.9) includes also half-integer powers of $\zeta - \mathrm{i}\chi_c$ because $\zeta = \mathrm{i}\chi_c$ is the square root branch the fpoint. Using equations (6.6) and (6.9) with the numerical values of $a_{-,1,2j}$, $j = 0, 1, 2, \ldots$, obtained as described in the beginning of this Section, one finds in the first sheet a numerical value of $z_{1,+,sum}(0)$ for each numerical value of χ_c. Then numerical Newton (secant) iterations are performed over χ_c aiming to ensure that $z_{1,+,sum}(0)$ converges to $\simeq z_{pade}(0)$, i.e. χ_c is chosen such that $z_{1,+,sum}(0)$ recovers the value of $z_{pade}(0)$. It provides χ_c with the precision at least 10^{-26} which is limited by the precision of Padé approximation. Part I also demonstrated the calculation of Stokes wave well beyond quad precision by using variable precision arithmetics with the achieved accuracy ~ 200 digits thus increasing of accuracy for χ_c is also possible if needed. Table 1 of Appendix C provides numerical values of χ_c which correspond to Padé approximations of Stokes wave found in Part I.

6.2. *Finding of $a_{+,2n+1,0}$ and $a_{-,2n,0}$ from matching the series expansions at $\zeta = \pm i\chi_c$ in the second, third etc. sheets*

The procedure for finding numerical values of χ_c and $a_{+,1,j}$, $j = 0, 1, 2, \ldots$ described in Section 6.1, together with equations (6.3) and (6.7), allows to immediately find $a_{-,2,j}$, $j = 1, 2, \ldots$ for each given value of $a_{-,2,0}$. Similar to equations (6.8) and (6.9), a notation is used such that $z_{l,+,sum}(\zeta)$ and $z_{l,-,sum}(\zeta)$ are the finite sums corresponding to the truncation of the series $z_{l,+}(\zeta)$ (6.1) and $z_{l,-}(\zeta)$ (6.2), respectively. We assume that $j_{max} \simeq 200$ for these finite sums in the sheets $l = 1, 2, \ldots$. The numerical Newton iterations at the first step are performed over $a_{-,2,0}$ aiming to ensure that $z_{2,-,sum}(0)$ converges to $z_{2,+,sum}(0)$. At the second step the Newton iterations allow to find $a_{+,3,0}$ by matching $z_{3,-,sum}(0)$ and $z_{3,-,sum}(0)$. In a similar way, the third, fourth etc. steps allow to find $a_{-,4,0}$, $a_{+,5,0}$, $a_{-,6,0}$, $a_{+,7,0}, \ldots$ Then using equations (6.7), one obtains values of $a_{+,n,0}$ and $a_{-,n,0}$ for all positive integer n completing the analytical continuation of Stokes wave into the disks $|\zeta \pm \mathrm{i}\chi_c| < 2\chi_c$ in the infinite number of sheets of Riemann surface.

The result of that analytical continuation was compared with the analytical continuation by ODE integration of Section 5 giving the excellent agreement which is only limited by the standard numerical accuracy $\sim 10^{-26}$ of Stokes wave in physical sheet. Increasing that accuracy of analytical continuation is straightforward by increasing j_{max} for the finite sums $z_{l,+,sum}(\zeta)$ and $z_{l,-,sum}(\zeta)$ (and similar by increasing the accuracy for ODE integration) provided Stokes wave precision is increased. Table 2 of Appendix C provides a sample of numerical values of $a_{-,2n,0}$, $a_{+,2n+1,0}$, for $n = 1, 2, 3$ obtained by the numerical method outlined in this Section.

7. Singularities of Stokes wave for finite values of w

Grant (1973) and Tanveer (1991) showed that the only possible singularity in the finite complex upper half-plane of the physical sheet of Riemann surface is of square root type.

This result is consistent with with the simulations of Part I (Dyachenko *et al.* 2015*b*) and numerical integration of ODE (3.4) in Section 5.

The analysis of Tanveer (1991) is based on a version of equation (3.2) together with the assumption of the analyticity of $\bar{z}(w)$ in $\mathbb{C}^+$ for the fist sheet of Riemann surface. Assume that one performs ODE integration in the second, third etc. sheets of Riemann surface as described in Sections 5 and 6 with $z(w)$ at the nth sheet coupled to $\bar{z}(w)$ in the $n-1$th sheet. Here the counting of sheets follows Section 5 and assumes that $-\pi < Re(w) < \pi$, $|Im(w)| < \infty$ for all sheets. Then the analysis of Tanveer (1991) can be immediately generalized to the nth sheet at values of $w = w_1$ such that $z(w)$ has no singularity at $w = \bar{w}_1$ in the $n-1$th sheet. Coupling of square root singularities at $\zeta = \pm \mathrm{i}\chi_c$ which is studied in Section 6 however goes beyond the analysis of Tanveer (1991).

The series expansions of Section 6 show that square root singularities can occur at any finite values of $w = w_1$ away from the real axis. It was found in Section 6 that each square root singularity can either have a sister square-root singularity at the complex conjugated point $w = \bar{w}_1$ in the same sheet or can exists without the sister singularity at $w = \bar{w}_1$ thus going beyond the case analyzed by Tanveer (1991). A question still remains if any other type (beyond square root) of coupled singularities at $w = w_1$ and $w = \bar{w}_1$ in the same sheet is possible.

Going from the first sheet to the second one, then from the second one to the third one etc., one concludes that the only way for the singularity other than square root to appear is to be coupled with the square root singularity in the previous sheet. Otherwise if would violate the above mentioned generalization of the result of Tanveer to arbitrary sheet. Consider a general power law singularity of $z(w)$ at $w = w_1$ coupled with the square root singularity of $\bar{z}(w)$ at $w = \bar{w}_1$. We write that general singularity in terms of double series as follows

$$z(w) = \sum_{n,m} c_{n,m}(w - w_1)^{n/2+m\alpha}, \tag{7.1}$$

where α is the real constant, $c_{n,m}$ are complex constants and n, m are integers. By shifting n and m once concludes that without loss of generality one can assume that

$$0 < \alpha < 1/2. \tag{7.2}$$

After the complex conjugation, the square root singularity of $z(w)$ at $w = \bar{w}_1$ is given by the following series

$$\bar{z}(w) = \sum_{n=0}^{\infty} d_n(w - w_1)^{n/2}, \tag{7.3}$$

where d_n are the complex constants. Coupling of $z(w)$ and $\bar{z}(w)$ in equation (3.3) explains why half-integer powers $n/2$ must be taken into account in equation (7.1). It is convenient to transform from w into a new complex variable

$$q \equiv (w - w_1)^{1/2}. \tag{7.4}$$

Equation (3.3) for the new variable q takes the following form

$$z_q = \frac{4q^2c^2}{\bar{z}_q[\mathrm{i}(z - \bar{z}) + c^2]}. \tag{7.5}$$

The series (7.1) is then transformed into

$$z(q) = \sum_{n,m} c_{n,m} q^{n+2m\alpha}, \tag{7.6}$$

while the series (7.3) runs over integer powers,

$$\bar{z}(q) = \sum_{n=0}^{\infty} d_n q^n. \tag{7.7}$$

The series (7.6) can be also called by ψ-series, see e.g. Hille (1997). If α is the rational number then in equation (7.1) one can gather together all terms with the same power of q thus reducing equation (7.1) to Puiseux series

$$z(q) = \sum_{n=-\infty}^{\infty} \tilde{c}_n q^{2n/k}, \tag{7.8}$$

where k is the positive integer.

If one additionally restricts that there is no essential singularity at $q = 0$ then one has to replace (7.6) with the truncated series

$$z(q) = \sum_{n \geqslant n_0, m \geqslant m_0} c_{n,m} q^{n+2m\alpha}, \tag{7.9}$$

for the integer constants n_0 and m_0. Plugging in equations (7.7) and (7.9) into the Stokes wave equation (7.5), moving the denominator to the l.h.s. in equation (7.5) and collecting terms with the same power of q, starting from the lowest power, one obtains that 2α must be integer for any values of n_0 and m_0 and all values of d_n. Thus no new solutions in the form (7.9) exists beyond what was found in Section 6.

One can also study singularities using the classification of movable and fixed singularities in nonlinear ODEs of 1st order in the general form $z_q = f(q, z)$ (see e.g Golubev (1950); Hille (1997); Ince (1956)). Position of fixed singularities for the independent complex variable q is determined by the properties of ODE, i.e. by singularities of the function $f(q, z)$. In contrast, the position of movable singularity is not fixed but typically is determined by an arbitrary complex constant. To analyze singularities, it is convenient to introduce a new unknown

$$\xi(q) \equiv \frac{1}{\mathrm{i}(z - \bar{z}) + c^2}. \tag{7.10}$$

Then equation (7.5) takes the following form

$$\xi_q = \mathrm{i}\bar{z}_q \xi^2 - \frac{4\mathrm{i}q^2 c^2 \xi^3}{\bar{z}_q}, \tag{7.11}$$

where one reminds that $\bar{z}(q)$ is assumed to be known and is determined by $z(\bar{q})$ from the previous sheet of Riemann surface. Equation (7.11) has a cubic polynomial r.h.s in ξ which ensures that it has a movable square root singularity

$$\xi = \sum_{n=-1}^{\infty} c_n (q - C)^{n/2}, \tag{7.12}$$

provided $C \neq 0$, $\bar{z}_q(C) \neq 0$ (see e.g Golubev (1950); Hille (1997); Ince (1956)), where c_n and C are complex constants. Using equations (7.4), (7.10) and the condition $C \neq 0$, one recovers the expansion (7.3) with w_1 replaced by $w_1 + C^2$ thus the movable singularity (7.12) is reduced to square root singularity in w.

Equation (7.11) has a fixed singularity at $q = 0$ provided $\bar{z}_q(0) \neq 0$. To show that one uses a new unknown $\psi \equiv 1/\xi$ to transform equation (7.11) into

$$\psi_q = \frac{-\mathrm{i}\bar{z}_q^2\psi + 4\mathrm{i}q^2c^2}{\bar{z}_q\psi}, \tag{7.13}$$

which has 0/0 singularity in r.h.s. for $q = \psi = 0$ satisfying the criteria for the existence of fixed singularity (see Golubev (1950); Hille (1997)).

Consider now a particular case $\bar{z}_q(0) = 0$ and $\bar{z}_{qq}(0) \neq 0$ which corresponds to the expansion (6.3). One can define a new function

$$g(q) \equiv \frac{\tilde{z}_q}{q}, \quad g(0) \neq 0 \tag{7.14}$$

and rewrite equation (7.13) as follows

$$\psi_q = \frac{-\mathrm{i}qg(q)^2\psi + 4\mathrm{i}qc^2}{g(q)\psi}, \tag{7.15}$$

Generally this equation still has a fixed singularity because of 0/0 singularity in r.h.s.. However, in a particular case when $g(q)$ is the even function of q, i.e. one can define the function $\tilde{g}(q^2) \equiv g(q)$ which is analytic in the variable $\tilde{q} \equiv q^2$ at $q = 0$. This case means that $z(w)$ is analytic at $w = w_1$. Then one transforms equation (7.15) into the equation

$$\psi_{\tilde{q}} = \frac{-\mathrm{i}\tilde{g}(\tilde{q})^2\psi + 4\mathrm{i}c^2}{2\tilde{g}(\tilde{q})\psi}, \tag{7.16}$$

which does not have a fixed singularity. Equation (7.16) together with equation (7.12) reproduces the result of Tanveer (1991).

Thus the approaches reviewed in Refs. Golubev (1950); Hille (1997); Ince (1956) applied to equation (7.5) are consistent with square root singularities and the series expansions of Section 6 for all sheets of Riemann surface. However, these approaches cannot exclude the possibility of existence of other singularities. Note that examples given in Golubev (1950); Hille (1997); Ince (1956) also show that the existence of the fixed singularity in ODE at the point $q = 0$ does not necessary mean that the singularity occurs in the general ODE solution $z(q)$ at that point.

One concludes that a coupling of the essential singularity at $w = w_1$ with the square root singularity at $w = \bar{w}_1$ cannot be excluded by neither the series analysis used in equations (7.4)-(7.9) and nor by looking at the fixed ODE singularities through equations (7.10)-(7.15). However, the simulations of Section 5 and series expansions of Section 6 clearly indicates the absence of any singularities beyond square root at the distance less than v_c from the origin in all sheets of Riemann surface for non-limiting Stokes wave. It is conjectured here that such singularities do not appear in all sheets of Riemann surface for the general domain (stripe) $-\pi < Re(w) < \pi$, $|Im(w)| < \infty$.

As discussed at the end of Section 5, singularities are possible at the boundary of the strip $Re(w) = \pm\pi$ which corresponds to the branch cuts $[\mathrm{i}, \mathrm{i}\infty]$ and $[-\mathrm{i}, -\mathrm{i}\infty]$ in ζ plane. However, these branch cuts are separated by the distance π from the origin in w plane (or by the distance 1 in ζ plane) and they cannot explain the formation of limiting Stokes wave as $v_c \to 0$. The same is true for the singularity at $w \to \mathrm{i}\infty$ ($\zeta \to \mathrm{i}$) analyzed in Section 4.

8. Conjecture on recovering of 2/3 power law of limiting Stokes wave from infinite number of nested square root singularities of non-limiting Stokes wave as $\chi_c \to 0$

One concludes from Sections 6 and 7 that the only possibility for the formation of 2/3 power law singularity (1.1) of the limiting Stokes wave is through the merging together the infinite number of square-root singularities from different sheets of Riemann surface in the limit $v_c \to 0$. The total number of square-root singularities could be either finite of infinite for $v_c > 0$, both cases are compatible with the expansions of Section 6 (although the infinite number of singularities appears to hold for the generic values of the expansion coefficients of Section 6). Both numerical ODE integration of Section 5 and series expansions of Section 6 reveal that the number of sheets of Riemann surface related to singularities at $\zeta = \pm \mathrm{i}\chi_c$ exceeds several hundreds for a wide range of numerical values $0.2 \lesssim \chi_c \lesssim 10^{-7}$. It suggests that the number of sheets is infinite for all values of v_c. In any case, the number of singularities must be infinite as $v_c \to 0$.

Here a conjectured is made that the limiting Stokes wave occurs as the limit $v_c \to 0$ of the following leading order solution

$$
\begin{aligned}
z = {} & \mathrm{i}\frac{c^2}{2} + c_1 \chi_c^{1/6} \sqrt{\zeta - \mathrm{i}\chi_c} + \\
& + 3^{2/3} e^{\mathrm{i}\pi/3} \left[(\zeta - \mathrm{i}\chi_c)^{1/2} + (-2\mathrm{i}\chi_c)^{1/2} \right] \sqrt{\alpha_1 \chi_c^{1/4} + \sqrt{(\zeta - \mathrm{i}\chi_c)^{1/2} + (-2\mathrm{i}\chi_c)^{1/2}}} \\
& \times \sqrt{\alpha_3 \chi_c^{1/16} + \sqrt{\alpha_2 \chi_c^{1/8} + \sqrt{\alpha_1 \chi_c^{1/4} + \sqrt{(\zeta - \mathrm{i}\chi_c)^{1/2} + (-2\mathrm{i}\chi_c)^{1/2}}}}} \\
& \times \sqrt{\alpha_{2n+1} \chi_c^{1/2^{2n+1}} + \sqrt{\alpha_{2n} \chi_c^{1/2^{2n}} + \sqrt{\ldots + \sqrt{\alpha_1 \chi_c^{1/4} + \sqrt{(\zeta - \mathrm{i}\chi_c)^{1/2} + (-2\mathrm{i}\chi_c)^{1/2}}}}}} \\
& \times \cdots + \text{h.o.t.},
\end{aligned}
\tag{8.1}
$$

which is the infinite product of increasingly nested square roots. Here c_1, α_1, α_2, α_3, $\alpha_4, \ldots$ are nonzero complex constants of the order $O(1)$. At $\zeta \gg \chi_c$ one obtains from equation (8.1) using the asymptotic of products of all square roots that

$$
z \propto \zeta^{1/2 + 1/8 + 1/32 + 1/128 + \ldots} = \zeta^{2/3} \tag{8.2}
$$

exactly reproducing the Stokes solution (1.1) while the term $c_1 \chi_c^{1/6} \sqrt{\zeta - \mathrm{i}\chi_c}$ vanishes as $\chi_c \to 0$. For small but finite χ_c, the limiting Stokes solution (1.1) is valid for $\chi_c \ll \zeta \ll 1$, as seen from equation (8.1). For $\zeta \sim 1$, the higher order terms denoted by h.o.t. both in equations (1.1) and (8.1), becomes important such as the term with the irrational power

$$
\propto \zeta^{\mu}, \ \mu = 1.4693457\ldots \tag{8.3}
$$

(Grant 1973; Williams 1981).

Different branches of all square roots in equation (8.1) choose different sheets of Riemann surface following the numeration of sheets used in Section 5. In particular, the principal branch of $(\zeta - \mathrm{i}\chi_c)^{1/2}$ in the expression $g(\zeta) \equiv (\zeta - \mathrm{i}\chi_c)^{1/2} + (-2\mathrm{i}\chi_c)^{1/2}$ corresponds to the first sheet. To understand that one expands $g(\zeta)$ at $\zeta = -\mathrm{i}\chi_c$ which results

in

$$g_+(\zeta) = 2(-2\mathrm{i}\chi_c)^{1/2} + \frac{\zeta + \mathrm{i}\chi_c}{2(-2\mathrm{i}\chi_c)^{1/2}} + O(\zeta + \mathrm{i}\chi_c)^2, \tag{8.4}$$

where the subscript + means taking the principle branch of $(\zeta - \mathrm{i}\chi_c)^{1/2}$. For the second branch of $(\zeta - \mathrm{i}\chi_c)^{1/2}$ one obtains that

$$g_-(\zeta) = -\frac{\zeta + \mathrm{i}\chi_c}{2(-2\mathrm{i}\chi_c)^{1/2}} + O(\zeta + \mathrm{i}\chi_c)^2 \tag{8.5}$$

with the subscript − meaning that second branch.

The expression $g(\zeta)$ enters under the most inner square root into each term of the product in equation (8.1). Then using the expansion (8.4) one obtains that the series expansion of equation (8.1) contains only nonnegative integer powers of $\zeta + \mathrm{i}\chi_c$ thus confirming that $z(\zeta)$ is analytic at $\zeta = -\mathrm{i}\chi_c$. It means that the condition (6.5) is satisfied. In contrast, taking the expansion (8.5) one obtains that the series expansion of equation (8.1) is of the type (6.2) containing nonnegative half-integer powers of $\zeta + \mathrm{i}\chi_c$ as expected for all sheets starting from the second sheet. In addition, the term $g(\zeta)$ in the square brackets in equation (8.1) ensures that $a_{-,2n,1} = 0$ as required by equation (6.3).

The expansion of equation (8.1) at $\zeta = \mathrm{i}\chi_c$ has half-integer powers of $\zeta - \mathrm{i}\chi_c$ for both branches of $g(\zeta)$ thus being consistent with the square root singularity at $\zeta = \mathrm{i}\chi_c$ in all sheets of Riemann surface including the first sheet in agreement with equations (6.1), (6.4) and (6.6).

Choosing two possible branches of all other square roots (besides the most inner square root) in equation (8.1) one obtains the expansions (6.1) and (6.2), at $\zeta = \pm\mathrm{i}\chi_c$ with different coefficients $a_{+,l,j}$ and $a_{-,l,j}$ at each lth sheet. The values of these coefficients are determined by both values of χ_c, c_1, α_1, α_2, α_3, $\alpha_4, \ldots$ together with the contribution from h.o.t terms in equation (8.1). One concludes that the ansatz (8.1) is consistent with the properties of non-limiting Stokes wave studied in this paper which motivates the conjecture (8.1). Also coefficients α_1, α_2, $\alpha_3, \ldots$ determine additional square root branch points which are located away from the imaginary axis at distance larger than χ_c from the origin in the third and higher sheets of Riemann surface. Values of these coefficients can be determined from the locations of branch points thus independently recovered from ODE integration similar as described in Section 5.

9. Concluding remarks

In summary, it was found that the Riemann surface corresponding to non-limiting Stokes wave consists of the infinite number of sheets corresponding to the infinite number of square root branch points located at $\zeta = \pm\mathrm{i}\chi_c$ in all sheets expect the first sheet. The first (physical) sheet has only one singularity at $\zeta = \mathrm{i}\chi_c$ while avoiding singularity at $\zeta = -\mathrm{i}\chi_c$ which ensures that Stokes wave represents the analytical solution inside the fluid domain. Two ways of analytical continuation into all these sheets were used, the first one is based on ODE integration of Section 5 and the second one is based on the coupled series expansions (6.1)-(6.6) in half-integer powers at $\zeta = \pm\mathrm{i}\chi_c$.

To go beyond the disks of convergence $|\zeta \pm \mathrm{i}\chi_c| < 2\chi_c$ of series expansions (6.1)-(6.6), it is conjectured in Section 8 that the leading order form of non-limiting Stokes wave has the form of the infinite number of nested square roots (8.1). These nested square roots can recover the series expansions (6.1)-(6.6) within their disks of convergence $|\zeta \pm \mathrm{i}\chi_c| < 2\chi_c$. For $|\zeta \pm \mathrm{i}\chi_c| \gg \chi_c$, well beyond these disks of convergence, the asymptotic (8.2) is valid thus ensuring that the nested square roots form 2/3 power law singularity of the limiting Stokes wave in the limit $\chi_c \to 0$.

There is another infinite sequence of Riemann sheets resulting from the singularity at $\zeta = \mathrm{i}$ (corresponds to $w = \mathrm{i}\infty$) which involves logarithms as analyzed in Section 4. However, these sheets do not contribute to the the qualitative change of power law singularity from 1/2 (non-limiting Stokes wave) to 2/3 (limiting Stokes wave) near the origin as given by the asymptotic (8.2). However, these sheets corresponding to $\zeta = \mathrm{i}$ might be important for analysis of Stokes wave for $\zeta \sim 1$, where the higher order terms becomes important such as the term (8.3) with the irrational power (Grant 1973; Williams 1981). The analysis of these terms is however beyond the scope of this paper.

Appendix A. Equivalence of two form of equation for Stokes wave

In this Appendix we show that both forms (2.1) and (3.1) of equation for Stokes wave are equivalent to each other. Then Section 2 implies that equations (2.13) and (2.22) are also equivalent to equations (2.1) and (3.1). Equation (2.1) was obtained by Dyachenko *et al.* (1996) while equation (3.1) in slightly different forms was used by numerous authors including Grant (1973); Longuet-Higgins & Fox (1977); Schwartz (1974); Stokes (1880*b*); Williams (1981) and Tanveer (1991). Appendix B explains derivation of equation (3.1) starting from basic equations of the potential flow of ideal fluid with free surface.

Applying the Hilbert operator $\hat{H}$ (2.2) to equation (2.1) and using the relations (2.14) and (2.15) one obtains that

$$c^2 \tilde{x}_u - y x_u + \hat{H}[y y_u] = 0, \tag{A 1}$$

which is equivalent to equation (2.13). We define a new variable

$$f \equiv -\hat{H}[y y_u] \tag{A 2}$$

and split it into two functions

$$f = f^+ + f^-, \tag{A 3}$$

using equations (2.4), (2.8) and (2.9) such that f^+ and f^- are the functions which are analytic in upper half-plane $\mathbb{C}^+$ and lower complex half-plane $\mathbb{C}^-$ of w, respectively. Note that zeroth harmonic $f_0 = 0$ as follows from the definition (A 2). Taking the linear combination of f and $\hat{H}f$, using equations (2.1), (A 1) and (A 2), one finds that

$$x_u \hat{H} f + y_u f = c^2 \tilde{x}_u y_u. \tag{A 4}$$

Using obvious relations

$$x_u = \frac{1}{2}(z_u + \bar{z}_u), \quad y_u = \frac{1}{2\mathrm{i}}(z_u - \bar{z}_u) \tag{A 5}$$

together with equations (A 3), (2.10) one obtains from equation (A 4) that

$$\bar{z}_u f^+ - z_u f^- = \frac{c^2}{4}\left(\bar{\tilde{z}}_u^2 - \tilde{z}_u^2\right). \tag{A 6}$$

Recalling that z_u is analytic and in $\mathbb{C}^-$ and, respectively, $\bar{z}_u$ is analytic and in $\mathbb{C}^+$, we apply the projector (2.11) to equation (A 6) and find that

$$\begin{aligned} f^+ &= \frac{c^2}{4}\frac{\bar{\tilde{z}}_u^2}{\bar{z}_u}, \\ f^- &= \frac{c^2}{4}\frac{\tilde{z}_u^2}{z_u}, \end{aligned} \tag{A 7}$$

where $z_u \neq 0$ in $\mathbb{C}^-$ and $\bar{z}_u \neq 0$ in $\mathbb{C}^+$ because $z(w)$ is the conformal transformation in $\mathbb{C}^-$.

Then using equations (A 1), (A 2), (A 3), (A 5) and (A 7) with some algebra we recover equation (3.1) thus completing the proof of its equivalence to equation (2.1). Note that the zero mean elevation condition (2.15) is essential in that proof making equation (A 1) valid. Shifting of the origin in y-direction would result in the nonzero value of the mean elevation $y_0 \equiv \int_{-\pi}^{\pi} \eta(x,t)\mathrm{d}x$. Then one would have to replace y by $y - y_0$ in equation (3.1). E.g. Tanveer (1991) took $y_0 = -1/2$. A similar choice $y_0 = -1/2$ was used by Grant (1973) and Williams (1981) up to trivial scaling of parameters.

Appendix B. Stokes wave in the rest frame and in the moving frame

Starting from Stokes (1880*b*), it has been common to write Stokes wave equation at moving reference frame in transformed form with a velocity potential and a stream function used as independent variables, see e.g. Grant (1973); Williams (1981) and Tanveer (1991). The purpose of this Appendix is to relate that traditional form of Stokes wave equation to another form used by to Dyachenko *et al.* (1996); Zakharov *et al.* (2002).

In physical coordinates (x, y) a velocity $\mathbf{v}$ of two dimensional potential flow of inviscid incompressible fluid is determined by a velocity potential $\Phi(x, y, t)$ as $\mathbf{v} = \nabla\Phi$. Here x is the horizontal axis and y is the vertical axis pointing upwards. The incompressibility condition $\nabla \cdot \mathbf{v} = 0$ results in the Laplace equation

$$\nabla^2\Phi = 0 \tag{B 1}$$

inside fluid $-\infty < y < \eta(x,t)$. The Laplace equation is supplemented by the dynamic boundary condition (the Bernoulli equation at the free surface $y = \eta(x,t)$)

$$\left(\frac{\partial\Phi}{\partial t} + \frac{1}{2}\left(\nabla\Phi\right)^2\right)\Big|_{y=\eta(x,t)} + \eta = 0 \tag{B 2}$$

and the kinematic boundary condition

$$\frac{\partial\eta}{\partial t} = \left(-\frac{\partial\eta}{\partial x}\frac{\partial\Phi}{\partial x} + \frac{\partial\Phi}{\partial y}\right)\Big|_{y=\eta(x,t)} \tag{B 3}$$

at the free surface. In our scaled units the acceleration of gravity is $g = 1$. We define the boundary value of the velocity potential as $\Phi(x,y,t)|_{y=\eta(x,t)} \equiv \psi(x,t)$. Equations (B 1), (B 2) and (B 3), together with the decaying boundary condition at large depth

$$\Phi(x,y,t)|_{y\to-\infty} = 0 \tag{B 4}$$

form the closed set of equations. Equation (B 4) implies that the rest frame is used such that there is no average fluid flow deep inside fluid. See also Part I (Dyachenko *et al.* 2015*b*) for more details on basic equations of free surface hydrodynamics.

Consider the stationary waves moving in the positive x direction (to the right) with the constant velocity c so that

$$\begin{aligned} &\Phi = \Phi(x - ct, y), \\ &\eta = \eta(x - ct). \end{aligned} \tag{B 5}$$

It was obtained in Ref. Dyachenko *et al.* (1996) (see also Part I (Dyachenko *et al.* 2015*b*)) that $\Psi = -c\hat{H}y = c\tilde{x}$, where $\hat{H}$ is the Hilbert transform (2.2). Respectively,

$\hat{H}\Psi = cy$ and the complex velocity potential Π at the free surface is given by

$$\Pi = \Psi + i\hat{H}\Psi = c(x + iy - u). \tag{B 6}$$

The analytical continuation of (B 6) into the lower complex half-plane $w \in \mathbb{C}^-$ is given by

$$\Pi = c(z - w) = c\tilde{z}. \tag{B 7}$$

We perform a Galilean transformation to a frame moving with the velocity c in the positive direction with the new horizontal coordinate $x' \equiv x - ct$ so that the velocity potential and the surface elevation turn time-independent as $\Phi(x')$ and $\eta(x')$, respectively. Alternatively, one can also define a velocity potential in the moving frame as $\tilde{\Phi}(x', y) = \tilde{\Phi}(x - ct, y)$ such that

$$\Phi = (x - ct)c + \tilde{\Phi}(x - ct, y). \tag{B 8}$$

Then equation (B 2) results in

$$\frac{1}{2}\left(\nabla\tilde{\Phi}\right)^2\Big|_{y=\eta(x-ct)} + \left(\eta - \frac{c^2}{2}\right) = 0 \tag{B 9}$$

and (B 3) gives

$$\left(-\frac{\partial\eta}{\partial x}\frac{\partial\tilde{\Phi}}{\partial x} + \frac{\partial\tilde{\Phi}}{\partial y}\right)\Big|_{y=\eta(x-ct)} = 0. \tag{B 10}$$

The decaying boundary condition (B 4) is replaced by

$$\tilde{\Phi}(x', y)|_{y\to-\infty} = -c. \tag{B 11}$$

Equations (B 9), (B 10) and (B 11) are the standard equations for Stokes wave in the moving frame, see e.g. Grant (1973); Williams (1981). Often small variations of equations (B 9), (B 10) and (B 11) are used such as a trivial shift of the origin in the vertical direction $\eta - \frac{c^2}{2} \to \eta$, assuming that Stokes wave moves in negative direction (to the left) and rescaling c to one (then the spatial period 2π is also rescaled) as was done in Grant (1973).

Similar to (B 8), we define the stream function in two forms, $\Theta(x')$ and $\tilde{\Theta}(x')$, as follows

$$\Theta = c\,y + \tilde{\Theta}(x - ct, y). \tag{B 12}$$

Using equations (B 8) and (B 12) one obtains that correspondingly two forms of the complex velocity potential, $\Pi(x')$ and $\tilde{\Pi}(x')$, are given by

$$\Pi = \Phi + i\Theta = cz - c^2t + \tilde{\Phi} + i\tilde{\Theta}. \tag{B 13}$$

A comparison of (B 7) and (B 13) reveals that

$$\tilde{\Pi} = \tilde{\Phi} + i\tilde{\Theta} = -c(w - ct) = -cw', \tag{B 14}$$

where $w' \equiv w - ct$. Thus $\tilde{\Pi}$ is the same as w' (up to the multiplication on $-c$) which explains why using the velocity potential $\tilde{\Phi}$ and the stream function $\tilde{\Theta}$ as independent variables in Refs. is equivalent to using w' as the independent variable in Ref. Dyachenko *et al.* (1996). The difference between Π and $\tilde{\Pi}$ is reflected by the boundary conditions (B 4) and (B 11) such that for Π the fluid at infinite depth has a zero velocity while for $\tilde{\Pi}$ that velocity is $-c$ in the x-direction. A technical advantage of working with Π instead of

Wave height H/λ	Singularity position χ_c
0.1004267517252848585467351563524 9	0.1212685583274560806968545972099 1
0.1206315745710018121117148609691 6	0.0504665130020465553400851062515 97
0.1400303773553623202432782785751 4	0.0007999065189780408034349632263817
0.1401510130643916461298866368093 0	0.0006516421043434869857704848281160 6
0.1403340478206115451239208500589 4	0.0004508756621296172724326390950681 8
0.1405141693862442761042173829795 9	0.0002842782236492223669017798017016 3
0.1405658442065383544497791168520 3	0.0002425254140881295695663014711328 4
0.1407085011062962082878982295720 3	0.0001419962749745755925401801770283 3
0.1407470301304427277948372028271 8	0.0001186840254544079015759929860694 5
0.1407566253261805001643951640120 3	0.000113140288627690141178081060480 8
0.1407774881851758036814780800093 4	0.000101451739666806817711755656376 62
0.1408083152523191676927256232191 3	0.000085108686515454366575393860892637
0.1408314037128099187221778352376 4	0.000073606496213860270898473095913984
0.1408507273198241157753139966765 0	0.000064475962982549833303295412314089
0.1408682599033785456534664292213 3	0.000056590609636696915090898733019878
0.1408779276527070996923633693375 8	0.000052407693639245443288926796396 85
0.1408858619711013363118830912722 4	0.000049063815868419517646209932713057
0.1408963510920997733690982457733 0	0.000044768056601363119620645100524 87
0.1409100170991052306264875194550 6	0.000039388011825703454833655362993012
0.1409183930755512840281296569555 3	0.000036214071851881467799287017287358
0.1409203262505150784437674474070 87	0.000035495061332908112086947410932 95
0.1409225244234177663005742886071 8	0.000034683708903596969054828355411 2
0.1409251475787555152545813124141 6	0.000033724196620161039218316518297236
0.1409273818063777076810709278025 1	0.000032914454078339616366407901860458
0.1409305690682372842611776972797 4	0.000031771329157192593064752326105744
0.1409351013719414374306126404889 8	0.000030170328722091325606940040468 7
0.1409411943069693719841666573901 4	0.000028063945797678144251500481216356
0.1409486782178318824034994466805 3	0.000025549865907771481807832323273915
0.1409535270747997941980095405212 9	0.000023964796260036642282422099761643
0.1409577893550459576441182528153 0	0.000022600407539173053002286018858435
0.1409700956571876687595010406375 2	0.000018816656490602043348418618380363
0.1409840766374872749646256787882 3	0.000014809683553364036868583695738714
0.1410015315485488955106417169048 4	0.000010273655389226364040855903301072
0.1410336511167120457180998559740 4	3.501228897483451227343779325593 9e-6
0.1410543164835804872851460684931 3	6.052003544391353606447974520920 7e-7
0.1410577788548832081649286022569 6	2.969122099463929109402884663423 7e-7

TABLE 1. A sample of numerical values of χ_c vs. the Stokes wave height H/λ.

$\tilde{\Pi}$ in Ref. Dyachenko *et al.* (1996) is that the decaying boundary condition (B 4) allows to relate real and imaginary parts of Π through the Hilbert transform for real values of w' as $\Theta = \hat{H}\Phi$ and $\Phi = -\hat{H}\Theta$. Equations (B 9) and (B 14) results in Stokes wave equation in the form (3.1) after we notice that $(\nabla\tilde{\Phi})^2|_{y=\eta} = \frac{|\tilde{\Pi}_u|^2}{|z_u|^2} = \frac{c^2}{|z_u|^2}$.

Appendix C. Table for numerical values of χ_c for Stokes wave

Table 1 provides the dependence of the singularity position χ_c on the scaled wave height H/λ for Stokes wave. Numerical values of χ_c are obtained by the numerical procedure described in Section 6.1. The Padé approximants from Part I (these approximants are also available at Dyachenko *et al.* (2015*a*)) are used for each values of H/λ. The accuracy of numerical values of χ_c is at least 10^{-26} which is limited by the precision of Padé approximation. Table 2 provides a sample of numerical values of $a_{-,2n,0}$ and $a_{+,2n+1,0}$ for four different values of χ_c corresponding to table 1. These numerical values of χ_c are

	$\chi_c = 0.12126\ldots$	$\chi_c = 0.05046\ldots$	$\chi_c = 0.000242\ldots$	$\chi_c = 2.969\ldots \times 10^{-7}$
$a_{-,2,0}$	1.947517181530394	1.332875450393561	0.616114648091185	0.5967616372529635
$a_{+,3,0}$	1.933089192507101	1.395722669719572	0.6227276830074182	0.5968472222666076
$a_{-,4,0}$	2.823744469669705	1.830765178354924	0.630550992725188	0.5969268580437934
$a_{+,5,0}$	2.715883020102187	1.841263995239744	0.6356646908933044	0.5969952862738779
$a_{-,6,0}$	3.541346294820654	2.238582675537623	0.642377214720984	0.5970622067844041

TABLE 2. A sample of numerical values of $a_{-,2n,0}$ and $a_{+,2n+1,0}$, $n = 1, 2, 3$, for different χ_c. More accurate numerical values of χ_c can be recovered from table 1.

obtained by the numerical procedure described in Section 6.2. For brevity only 16 digits of the numerical precision are shown.

REFERENCES

AMICK, C. J., FRAENKEL, L. E. & TOLAND, J. F. 1982 On the Stokes conjecture for the wave of extreme form. *Acta Math.* **148**, 193–214.

DYACHENKO, ALEXANDER I., KUZNETSOV, EVGENII A., SPECTOR, MICHAEL & ZAKHAROV, VLADIMIR E. 1996 Analytical description of the free surface dynamics of an ideal fluid (canonical formalism and conformal mapping). *Phys. Lett. A* **221**, 73–79.

DYACHENKO, SERGEY A., LUSHNIKOV, PAVEL M. & ALEXANDER O. KOROTKEVICH, HTTP://STOKESWAVE.ORG 2015*a* .

DYACHENKO, SERGEY A., LUSHNIKOV, PAVEL M. & KOROTKEVICH, ALEXANDER O. 2014 The complex singularity of a Stokes wave. *JETP Letters* **98** (11), 675–679.

DYACHENKO, SERGEY A., LUSHNIKOV, PAVEL M. & KOROTKEVICH, ALEXANDER O. 2015*b* Branch cuts of stokes wave on deep water. Part I: Numerical solution and Padé approximation to recover branch cut. *arXiv:1507.02784* .

DYACHENKO, SERGEY A., LUSHNIKOV, PAVEL M. & VLADIMIROVA, NATALIA 2013 Logarithmic scaling of the collapse in the critical Keller-Segel equation. *Nonlinearity* **26**, 3011–3041.

GOLUBEV, V. V. 1950 *Lectures on the Analytic Theory of Differential Equations (in Russian)*. Moscow: Gosud. Izd. Techniko-Teor. Leterat.

GRANT, MALCOLM A. 1973 The singularity at the crest of a finite amplitude progressive Stokes wave. *J. Fluid Mech.* **59(2)**, 257–262.

HILLE, E. 1997 *Ordinary Differential Equations in the Complex Domain*. Dover.

INCE, EDWARD L. 1956 *Ordinary Differential Equations*. Dover.

LONGUET-HIGGINS, M. S. & FOX, M. J. H. 1977 Theory of the almost-highest wave: the inner solution. *J. Fluid Mech.* **80(4)**, 721–741.

LUSHNIKOV, PAVEL M., DYACHENKO, SERGEY A. & VLADIMIROVA, NATALIA 2013 Beyond leading-order logarithmic scaling in the catastrophic self-focusing of a laser beam in Kerr media. *Phys. Rev. A* **88**, 013845.

PLOTNIKOV, P.I. 1982 A proof of the Stokes conjecture in the theory of surface waves. *Dinamika Splosh. Sredy (In Russian. English translation Stud. Appl. Math.3, 217-244 (2002))* **57**, 41–76.

SCHWARTZ, LEONARD W. 1974 Computer extension and analytic continuation of Stokes' expansion for gravity waves. *J. Fluid Mech.* **62(3)**, 553–578.

STOKES, GEORGE G. 1847 On the theory of oscillatory waves. *Transactions of the Cambridge Philosophical Society* **8**, 441–455.

STOKES, GEORGE G. 1880*a* On the theory of oscillatory waves. *Mathematical and Physical Papers* **1**, 197–229.

STOKES, GEORGE G. 1880*b* Supplement to a paper on the theory of oscillatory waves. *Mathematical and Physical Papers* **1**, 314–326.

TANVEER, S. 1991 Singularities in water waves and Rayleigh-Taylor instability. *Proc. R. Soc. Lond. A* **435**, 137–158.

Williams, J. M. 1981 Limiting gravity waves in water of finite depth. *Phil. Trans. R. Soc. Lond. A* **302(1466)**, 139–188.

Zakharov, Vladimir E., Dyachenko, Alexander I. & Vasiliev, Oleg A. 2002 New method for numerical simulation of nonstationary potential flow of incompressible fluid with a free surface. *European Journal of Mechanics B/Fluids* **21**, 283–291.